The Pennsylvania State University

The Graduate School

The College of Earth and Mineral Science

THE EFFECTS OF HYDROGEN ADDITION ON A SPARK-IGNITED COMPRESSED NATURAL GAS VEHICLE

A Thesis in

Energy and Geo-Environmental Engineering

by

Jamie Michael Clark

Submitted in Partial Fulfillment
of the Requirements
for the Degree of

Master of Science

May 2008

The thesis of Jamie Michael Clark was reviewed and approved* by the following:

André L. Boehman
Professor of Fuel Science and Materials Science and Engineering
Thesis Advisor

Sarma V. Pisupati
Associate Professor Energy and Mineral Engineering

Joel R. Anstrom
Research Associate, Pennsylvania Transportation Institute

Yaw D. Yeboah
Professor of Energy and Mineral Engineering
Head of the Department of Energy and Mineral Engineering

*Signatures are on file in the Graduate School

ABSTRACT

The “Freedom Car” Initiative enacted by the Bush Administration has placed significant emphasis on the development of a hydrogen economy in the United States. While hydrogen fuel-cell vehicles have been the focus of recent media attention, near term implementation of hydrogen as a combustion enhancer is a more reliable pathway for wide-scale hydrogen utilization within the next ten years. Through combustion analysis, hydrogen addition to natural gas has shown to increase thermal efficiency and reduce CO, NO and hydrocarbon emissions (UHC) in studies on stationary test cell engines. On-road vehicle studies testing hydrogen-natural gas blends show emissions benefits and increase in fuel economy. However, on-road tests lack exhaustive combustion analysis to explain what is occurring in the cylinder. In this study, the effect of a 33 percent volumetric blend of hydrogen (HCNG) on natural gas combustion was investigated in a 5.4L spark-ignited engine in a Ford E-250 van. In-cylinder combustion analyses were performed and untreated exhaust emissions were measured at 15 and 30 mph with road loads of 10, 20 and 30 horsepower. Hydrogen increased the flame speed reducing time for flame kernel development and combustion duration. However, the hotter burn lost more heat to the surroundings and thermal efficiency of HCNG was lower than natural gas. Increasing engine speeds magnified reduction in combustion duration created by hydrogen. As load on the engine increased, hydrogen-influenced reduction on burn time was reduced. Heat and throttling losses reduced the thermal efficiency of the combustion. More complete combustion with hydrogen reduced carbon-based emissions and bulk cylinder temperature increase drove increased NO formation.

TABLE OF CONTENTS

LIST OF FIGURES

LIST OF TABLES

ACKNOWLEDGEMENTS

I would like to thank my thesis adviser, Dr. André Boehman, for offering me the opportunity to join his group. I greatly appreciated his support, guidance and patience throughout the process of this study. I would also like to thank my committee members, Dr Anstrom, Dr. Pisupati and Dr. Yeboah, for reviewing my thesis.

I would like to give special thanks to Vince Zello for his technical help on the engine instrumentation. Without his assistance my data would never have been collected or been correct. Dr. Joel Anstrom, Sam Entz, and the mechanics of the PTI garage have given me great support in vehicle technology. Thanks to Jim Flanagan for letting me use his work vehicle. Also, Semtech-DS deserves thanks for performing an emissions measurement demonstration and giving me the emissions results.

I would like to thank Yu Zhang, Dr. Octavio Armas, and Dr. Thomas Litzinger for their support in troubleshooting heat release calculations. I would also like to thank Dr. Kirk Collier for his support in understanding the control of and changes to the van. Thanks also to Jeff Saxton for his help in signal processing. I'm grateful for Jim Szybist and Peter Perez for building the foundation of the LabVIEW heat release program. I am also grateful for everyone else not mentioned from the Diesel Combustion and Emissions Lab at the Energy Institute for their help and collaboration.

I am also grateful for the Government Automotive Transportation Education program for providing me financial support through my entire graduate school education.

Finally I would like to thank my wife and parents for their continued support for me and my life aspirations.

Chapter 1

Introduction

1.1 Motivation

Over the past decades natural gas has become a popular alternative fuel for the growing transportation sector. Light-duty vehicles running on natural gas represent a maturing technology, while natural gas heavy-duty transit vehicles are popular in urban areas. As a fuel source for large scale for transportation needs, natural gas provides advantages in automotive technology because of its emissions benefits in comparison with diesel and gasoline engines. The chemical structure of the fuel is advantageous as the carbon-hydrogen bonds in methane reduce carbon dioxide emissions per unit of energy compared diesel and gasoline.

However, there are several drawbacks with natural gas engines, particularly in efficiency and emissions as engines must meet increasingly stringent U.S. government-mandated requirements. Among hydrocarbons, methane, the main component in natural gas, has the slowest flame speed [1]. This reduces thermal efficiency by increasing energy losses due to heat transfer. Because of less efficient burning, significant amounts of methane remain in the exhaust after a combustion cycle is completed. The unburned methane expelled to the atmosphere can negate the fuels reduction in carbon dioxide emissions because it has 21 times the global warming potential [2] of carbon dioxide. Another issue in natural gas engines is maintaining proper engine control with varying

fuel composition. Hydrocarbon content in natural gas can vary, with the volumetric content of methane ranging from 70 to 96 percent. The Electronic Control Unit (ECU) adjusts the intake composition and spark timing based on an incorrect assumption of fuel energy, creating combustion conditions that reduce engine efficiency.

Other conditions which the natural gas vehicle industry must deal with include fuel storage, distribution, and safety issues. Fuel storage tanks require aggressive safety features such as stainless steel or carbon fiber tanks, which increase vehicle weight. Lack of appropriate gaseous fuel infrastructure prevents effective distribution to the entire population. Safety considerations sway public opinion which slows steps in research and development of this technology [3].

Despite these drawbacks and hindrances, some advances are being made in advocating the development of natural gas and alternative fuels. The "FreedomCAR (Cooperative Automotive Research)" initiative enacted in January 2002, as well as the Hydrogen Fuel Initiative announced by the Bush Administration in January 2003, places a significant emphasis on the development of the hydrogen economy (developing fuel cells and designing the necessary infrastructure for producing, storing, and distributing hydrogen) in the United States. While current technology and infrastructure does not lend itself to a commercial hydrogen economy, "hydrogen-assisted" combustion is a more realizable pathway for large-scale hydrogen utilization in the near future.

Despite the large amount of resources currently being devoted to hydrogen technology research, near-term implementation of hydrogen in the transportation sector is not yet a reality. To further research in this area and as part of The Pennsylvania State University's initiative towards a hydrogen economy, a partnership between the

university, Air Products, and Collier Technologies has resulted in the creation of hydrogen and hydrogen-compressed natural gas vehicles and a fueling station for use in university transportation and for research needs.

The potential of hydrogen to increase indicated thermal efficiency and reduce emissions in natural gas combustion has been investigated for several reasons. First, natural gas and hydrogen blend uniformly because they are both in a gaseous state at standard temperature and pressure. Hydrogen has a higher stoichiometric laminar flame speed in air than methane. Literature states [4] that an increase in laminar flame speed has been shown to reduce the flame initiation stage of combustion. This effect is even more pronounced at light-load conditions, where combustion duration is the longest. Another advantage of hydrogen is that it increases the stability of combustion at leaner burn mixtures, a characteristic that has been extensively researched in natural gas combustion. Finally, hydrogen and methane mixtures have been shown to slightly reduce pumping losses in the engine increasing the [5].

1.2 Objectives of Research

The objective of this research is to determine the in-cylinder combustion performance of natural gas and a hydrogen-natural gas blend in a vehicle equipped to operate using either fuel. The plan calls for the research vehicle to be run at a set vehicle speed and varying load conditions. The resulting combustion performance is measured to determine the effect of hydrogen on natural gas combustion. Hydrogen addition has been shown to have a positive effect on combustion and emissions in the literature, and

correlations will be drawn that evaluate if these hold true in the data obtained in this study. The hypothesis of this research is that, like in test cell engine research, hydrogen will decrease the combustion duration, increasing the indicated thermal efficiency of the engine, while reducing carbon monoxide and unburned hydrocarbons emissions. Increased gas temperatures will increase NO output.

1.3 Summary of Tasks

Due to the compactness of the efficient modern day vehicle, data acquisition instrumentation hardware had to be built around tightly packaged engine components. Hardware to measure in-cylinder pressure and crank angle position were purchased, designed, fabricated, and mounted onto the vehicle. The vehicle itself was mounted on a chassis dynamometer and run at set speeds and loads using compressed natural gas (CNG) and a 33 percent blend of hydrogen with compressed natural gas (HCNG). A data acquisition program was written in LabVIEW to record real-time cylinder pressures, while emissions data were simultaneously recorded using Sensors Inc.'s Semtech-DS emissions analyzer. Using a heat release calculation program written in Matlab, the combustion and emissions data were analyzed to determine combustion performance across all test points.

Chapter 2

Literature Review and Background

2.1 Outline

To gain insight into how hydrogen affects natural gas combustion in an internal combustion engine, it is essential to have a clear understanding of the fuel structure and properties of methane and hydrogen, as well as of spark-ignition combustion principles, differences in kinetic interactions, and vehicle loading. In this chapter, a description of the chemical structure and properties of methane and hydrogen is given, followed by an overview of the spark-ignited engine combustion process, combustion propagation mechanisms, and the quantitative ways in which combustion is measured. Finally, previous research on hydrogen's effect on natural gas combustion in engines and vehicles is reviewed.

2.2 Chemical Structure and Properties of Methane and Hydrogen Fuels

Natural gas is a light hydrocarbon composed of methane (CH_4) and from 0 to 20 percent of ethane (C_2H_6) and propane (C_3H_8). Nitrogen, helium, and carbon dioxide are also found in trace amounts. Natural gas has the highest ignition temperature of any commonly used hydrocarbon fuel, and is the slowest burning as well [6].

While engine manufacturers have produced engines that run on compressed natural gas (CNG), a more recent development is conversion of engines to operate on a

hydrogen-natural gas blend fuel, which is commonly known as hydrogen enriched compressed natural gas, or HCNG. By displacing some natural gas with hydrogen, scientists and engineers have been attempting to improve combustion performance and extend the lean-burn limit of methane, by blending 1 to 30 volume percent hydrogen in natural gas. This process has generated enough interest that one company, Hythane Company LLC, has patented a 20 volume percent blend of hydrogen with natural gas labeled “Hythane”.

Hydrogen addition has been shown to increase thermal efficiency and reduce carbon monoxide and unburned hydrocarbons by increasing the combustion quality of natural gas [5]. Table 2-1 compares the fuel characteristics of hydrogen and methane:

Table **2-1**: Hydrogen and Methane Fuel Properties [1]

	Hydrogen (H_2)	Methane (CH_4)
Equivalence Ratio ignition lower limit	0.10	0.53
Mass Lower Heating Value	119,930	50,020
Density of gas at STP (kg/m^3)	0.083764	0.65119
Volumetric Lower heating Value at STP (kJ/m^3)	10,046	32,573
Stoichiometric Air/Fuel Ratio	34.20	17.19
Volumetric Lower Heating Value in air at stoichiometric conditions (kJ/m^3)	2913	3088
Hydrogen to Carbon Ratio	0.00	0.25

Because of hydrogen’s highly reactive nature, it burns faster and more completely than methane. While this property makes hydrogen a prime candidate for increasing overall efficiency and reducing emissions, hydrogen is also less dense. Its displacement of natural gas in the fuel reduces the in-cylinder energy content, reducing power in a

volumetrically equivalent charge of natural gas. The very low volumetric energy density of hydrogen is one of hydrogen's major drawbacks.

2.2.1 Hydrogen Production

Hydrogen is a common element found in many naturally occurring substances, yet diatomic hydrogen (H_2) is not found naturally on earth. Hydrocarbon fuels (C_xH_y) and water (H_2O) are the primary sources for hydrogen production. Through a variety of energy intensive processes, primary energy sources such as coal, petroleum, and natural gas are refined into synthesis gas, as shown as in Eq. 2-1, to produce hydrogen. Another method used to produce pure hydrogen is to pass electric current through water to separate its hydrogen and oxygen atoms. Hydrogen offers an advantage over fossil fuels because there are multiple pathways for hydrogen production.

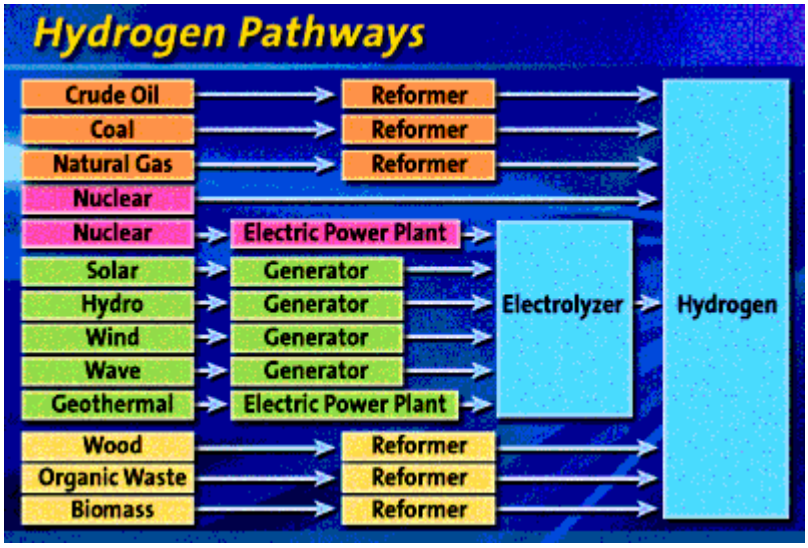

Figure **2-1**: Pathways to Hydrogen Production [7]

The most mature technology used to produce hydrogen is steam reforming of natural gas. Steam methane reforming (SMR) involves passing steam and natural gas over a nickel catalyst at temperatures above 500°C. The two reversible reactions responsible for hydrogen production are as follows.

$$CH_4 + H_2O \rightarrow CO + 3H_2 \text{ -49 kcal/mol} \quad \textbf{2.1}$$

$$CO + H_2O \rightarrow CO_2 + H_2 \text{ +10 kcal/mol} \quad \textbf{2.2}$$

During the process, steam is added in excess of the stoichiometric requirement so that Eq. 2.2 will shift right to form hydrogen and carbon dioxide [8]. The Pennsylvania State University uses a variant of this hydrogen-production strategy. This advanced steam methane reformer is the most cost-effective hydrogen producer for small-scale applications.

A pressure swing absorption (PSA) unit purifies the resulting gas to 99.99 percent pure hydrogen, which is compressed and stored [9]. The purified hydrogen is then recombined with unrefined natural gas to produce HCNG. In comparison to the price of pure natural gas, the cost of 80/20 and 90/10 blends of natural gas and hydrogen is 8 percent and 15 percent greater, respectively[10].

2.3 Fundamentals of Combustion in Spark-ignited Engines

In order to better understand the role that hydrogen plays in combustion, it is necessary to review the fundamentals of combustion in spark-ignited engines. In general, the natural gas spark-ignited engine combustion process can be summarized as follows.

At a suitable time during the intake stroke, gaseous fuel is introduced at a high pressure into the engine cylinder by the fuel injection system through small orifices. The fuel then mixes with throttled air coming in through the intake manifold. A few crank angle degrees of rotation before the piston reaches the top dead center (TDC) position, the air-fuel mixture ignites when the spark plug initiates combustion in the cylinder, causing the cylinder pressure and temperature to increase rapidly. As the piston moves further into the expansion stroke, the cylinder pressure and temperature begin to decrease. The combustion reactions are quenched as the cylinder temperature drops during the expansion stroke. Details of the spark-ignited engine combustion process are introduced in the following sections.

2.3.1 Spark-Ignited Stoichiometric Combustion of Hydrocarbons

Combustion is a rapid chemical reaction between radicals that converts chemical energy in the fuel to thermal energy via oxidation [6]. Assuming that only major products are formed, hydrocarbon fuels combust following the basic formula under stoichiometric conditions.

$$C_x H_y + a(O_2 + 3.76N_2) \rightarrow xCO_2 + \frac{y}{2} H_2O + 3.76aN_2 \qquad \textbf{2.3}$$

The stoichiometric air-fuel ratio can be found by taking the ratio of the mass of air to fuel using Eq. 2.4 with Eq. 2.3.

$$(A/F)_{stoich} = \frac{4.76a}{1} \frac{MW_{air}}{MW_{fuel}} \qquad \textbf{2.4}$$

When the mass of fuel and air is adjusted, the mixture can be considered fuel lean or fuel rich, and the change is indicated by the equivalence ratio. The equivalence ratio is the ratio between the stoichiometric air-fuel ratio and the actual air-fuel ratio.

$$\Phi = \frac{(A/F)_{stoich}}{(A/F)_{actual}} \qquad \textbf{2.5}$$

2.3.2 Flame Kernel Development

Before combustion can take place, a source of energy must first be introduced. In a spark-ignited engine, a spark plug initiates combustion, which develops the initial flame kernel. The energy input is enough to sustain a propagating flame, which in the first few crank angle degrees exhibits characteristics of a laminar flame. This smooth, spherical flame, which contains only minor irregularities, surrounds the spark plug gap.

Because of the smooth shape of the flame, the flame kernel development is highly sensitive to variations in laminar flame speed and mixture composition. Reduction in the flame speed causes heat to be lost by conduction to the surroundings, which leads to cooler flame temperatures. With lower flame temperatures, the flame kernel development process approaches the point of extinction and increased formaldehyde formation [11].

As the flame grows, it interacts with the turbulent flow field near the spark plug. Because of distinct, uncontrollable variations in the turbulence, the flame rarely propagates the same way in each cycle, causing cycle-to-cycle variation. Repetitive variation in the cylinder can lead to early flame quenching and reduced combustion performance. Once the flame kernel has developed into a turbulent flame, the most

significant parameter controlling the remaining flame propagation is the turbulent-kinetic energy in the cylinder [12].

2.3.3 Combustion Kinetics

Combustion is governed by radical intermediates when reacted with air. Radicals require high temperature to form. These temperatures are maintained during the reaction by heat produced by combustion. Radicals initiate a chain reaction, propagating the radical formation throughout the system. The first step in the combustion reaction is the chain-initiating step in which two stable molecules collide to form a stable molecule and two radicals. Next, chain propagating and branching steps involve the collision between a radical and stable molecules resulting in the formation of one or two radicals. Combustion is terminated when the radical pool is depleted by interactions of the radicals with the wall or through recombination. The next sections will explore the kinetics involved in methane and hydrogen combustion, to get an idea of why hydrogen benefits combustion on a molecular level.

2.3.4 Methane Oxidation Kinetics

In HCNG combustion, the two primary types of oxidation reactions involve methane and hydrogen. This section will explore the theories behind the changes in oxidation process.

The first step in the combustion of methane and air is the cleavage of a carbon-hydrogen bond, resulting in the creation of a hydrogen radical and a hydrocarbon radical.

The carbon-hydrogen bond in methane has approximately 40 kilojoules more energy than the same bond in long-chain hydrocarbons, leading to difficulty in methane-air ignition. More energy is required to break the first bond in the molecule, to initiate the reaction. The chain initiation reactions for combustion, shown below, are classified as either low-temperature or high-temperature reactions [6].

$$CH_4 + O_2 \rightarrow CH_3 + HO_2 \text{ (low temperature)} \quad \textbf{2.6}$$

$$CH_4 + M \rightarrow CH_3 + H + M \text{ (high temperature)} \quad \textbf{2.7}$$

2.3.5 Hydrogen Oxidation Kinetics

In the hydrogen-oxygen reaction system, the dissociation energy of hydrogen is lower than that of oxygen. In hydrogen oxidation, early forming H radicals advance combustion in the early stages of the burn. The literature [6] suggests that the chain-initiating step for hydrogen combustion, is the following:

$$H_2 + O_2 \rightarrow HO_2 + H \text{ (low temperature)} \quad \textbf{2.8}$$

It is argued that because of its high energy requirement, 435 kJ/mol, hydrogen will react only at high temperatures during a collision with another molecule, as in Eq. 2.9.

$$H_2 + M \rightarrow 2H + M \text{ (high temperature)} \quad \textbf{2.9}$$

The pool of O, H, and OH radicals builds quickly through a series of chain reactions:

$$H + O_2 \rightarrow O + OH \quad \textbf{2.10}$$

$$O + H_2 \rightarrow H + OH \quad \textbf{2.11}$$

$$O + H_2O \rightarrow OH + OH \quad \textbf{2.12}$$

These chain-branching reactions have very low activation energy, which advances combustion rapidly at lower temperatures.

2.4 Measuring Combustion Performance

Combustion statistics can be computed from the in-cylinder pressure measurements. Such statistics are useful in comparing combustion performance regardless of engine size, conditions, or as in the subject of this study, fuel.

Measured cylinder pressure in an internal combustion engine is a function of cylinder volume change, combustion, heat transfer to the cylinder walls, flow in and out of crevice regions, and flow past the piston rings. Pressure measurements are used to determine the approximate heat released in the cylinder during the four-stroke cycle. These data allow trends in the combustion process to be determined.

This section will describe the approach used to analyze the cylinder pressure and its use in determining the speed at which combustion occurs in the cylinder.

2.4.1 Mass Fraction Burned

Using pressure trace analysis to determine the fraction of the fuel burned in the cylinder as a function of crank angle allows for the characterization of the various stages of the combustion process and to compare rates of oxidation [11]. While a popular method to determine mass fraction burned is to use the Weibe function, it is also possible to approximate the fraction of fuel burned by using the normalized values of cumulative heat release. It must be taken into account that normalized heat release at stoichiometric

or rich conditions begins to deviate from the actual mass fraction burned, as shown in the modeled data in Figure **2-2**.

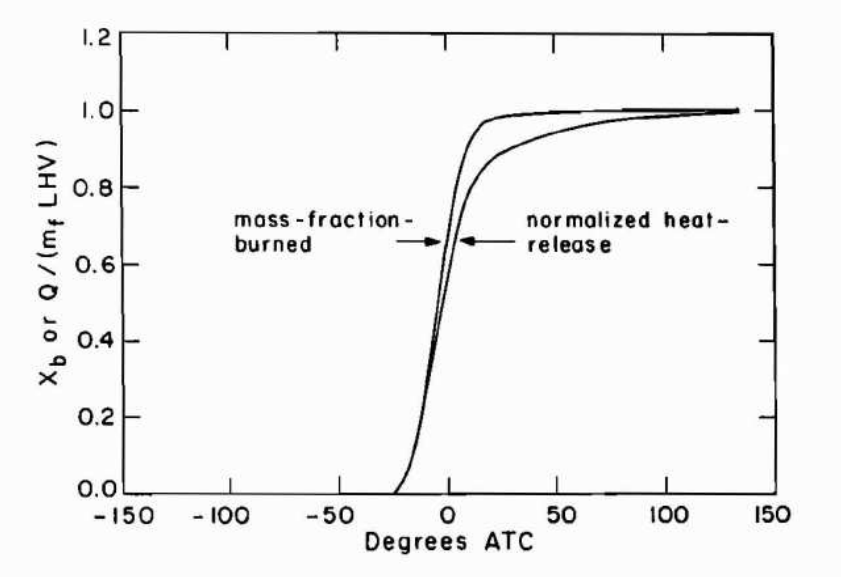

Figure **2-2**: Normalized Heat Release and Mass fraction burned [13]

Not all of the chemical energy of the burned fuel is released because of dissociation and limited oxygen availability, at high temperature and pressure conditions, resulting in the discrepancy shown above. The unconverted chemical energy is approximated by the enthalpy of CO and H_2 within the cylinder. Chun et al. [13] state that in real-time pressure data, normalized heat release is a reasonable estimate of mass fraction burned because the dissociation level will be smaller due to the effects of heat transfer and crevice losses on peak temperature. For the purposes of this study, the normalized heat release determined by the heat release data will equal the percent mass fraction burned of the fuel.

2.4.2 Ignition Delay

In a combustion chamber, ignition delay is governed by the chemistry of the fuel, the geometry of the combustion chamber, the air-fuel ratio, and cycle-to-cycle variations of combustion. Engine geometry and spark plug position dictate the flame front surface area. The larger the area, the more fresh charge can enter and propagate the combustion reaction. Also known as flame development angle, ignition delay is the crank angle interval from spark discharge to when a significant amount of fuel chemical energy has released. This quantity is usually 10 percent of fuel mass fraction burned, but can also be taken as 1 or 5 percent [11].

Heat release is computed using the derivative of pressure trace as a function of crank angle. Small oscillations in pressure data can cause significant errors in heat release analysis. These oscillations are exacerbated at low rates of heat release. To reduce the effect of noise, the crank angle interval from spark timing to 10 percent mass fraction burned is defined as the flame development angle as used in Swain et al. [4].

2.4.3 Combustion Duration

Combustion duration is the crank angle interval of during which the fuel burns in the cylinder. This measurement is the interval between 10 to 90 percent of the fuel mass fraction burned. From a thermodynamic standpoint, the highest efficiency is achieved if all of the chemical energy was released when the piston was at top dead center. However, achieving such a combustion rate is not only impractical, but also would cause irreparable damage to the engine. Manipulating engine conditions to decrease combustion duration is

advantageous because it reduces heat losses in the engine. Engine speed is a major factor in combustion duration: a four-fold increase in speed will increase the combustion duration by a factor of 1.6 at stoichiometric conditions [11].

2.5 Hydrogen Benefits to Combustion

In the following section, the benefits of hydrogen addition to combustion of natural gas are reviewed. Hydrogen fuel chemistry, composition, and properties lend itself to an increased efficiency, flame speed, and radical formation over those of methane during combustion.

2.5.1 Increased Cycle Efficiency

The theoretical maximum of a constant volume cycle conversion of fuel energy to usable energy is called the ideal cycle efficiency and is calculated by Eq. 2.13.

$$\eta_{i,CV} = 1 - \frac{1}{r_c^{\gamma-1}} \qquad \textbf{2.13}$$

Ideal cycle efficiency is a function of compression ratio and specific heat ratio (γ). Specific heat ratio is a measurement of the degrees of freedom of a molecule—the more degrees of motion in the molecule, the larger the number of degrees of freedom. A diatomic molecule, like hydrogen (H_2), will have a higher ratio of specific heats at the same temperature and pressure than a 5-atom molecule, like methane (CH_4) [14]. Hydrogen at standard temperature and pressure has a ratio of specific heats of 1.4, while the ratio for methane is 1.3. The ideal cycle efficiency would be expected as more

hydrogen is added to the charge, based on Eq. 2.13. Efficiency of an internal combustion engine is shown in Figure **2-3** as a function of gamma and compression ratio.

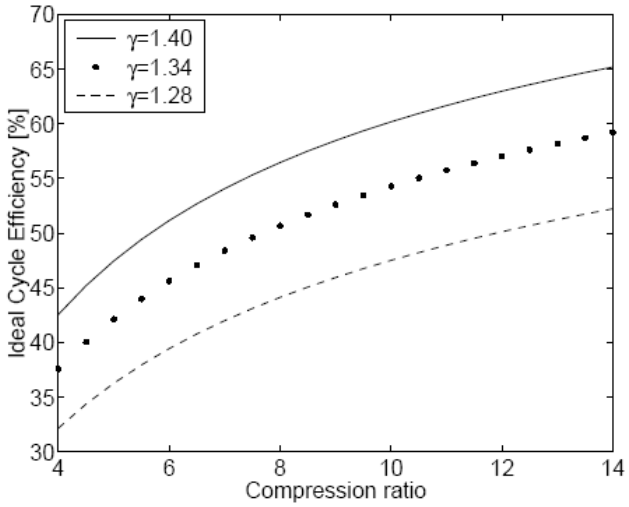

Figure **2-3**: Ideal cycle efficiency as a function of gamma and compression ratio[15]

One of the main sources of inefficiency in a spark-ignited engine is throttling of the intake airflow coming into the cylinder. Throttling results in less inducted air mass and an increased pressure drop as the air is drawn into the cylinder during the intake stroke. This reduces thermal efficiency because of a reduction in peak pressure attained during combustion. However, it has been shown [5] that a mixture of 20 percent hydrogen in natural gas when hydrogen blends are used, such pumping losses are reduced contributing to a higher thermal efficiency.

2.5.2 Increased Flame Speed

Quicker burn time reduces heat transfer from the hot in-cylinder gases to the surroundings, resulting in efficiency gains. During the faster combustion that occurs with

hydrogen and air, the thermal energy lost is only 17 to 25 percent of the total energy released. Methane air combustion loses 22 to 33 percent of its energy through the same convective heat transfer through the cylinder walls. The slower propagating flame speed of stoichiometric methane combustion in air is 40 cm/s while an identical hydrogen and air flame propagates at a rate between 265 and 325 cm/s [1]. Yu et al. [16] studied the effect of hydrogen addition to the flame speed of natural gas and found a linear correlation between the addition of hydrogen and the increase of the methane-hydrogen-air flame speed.

2.5.3 Rate-Limiting Factors

Because the process of combustion depends on the formation of radicals in order to accelerate flame propagation, a larger pool of radicals increases flame speed. However, some radical reactions have a slow reaction rate that governs the speed of combustion in the system. This reaction is known as the rate-limiting step because it controls how fast the overall reaction occurs.

It has been hypothesized by Collier et al. [17] that the rate-limiting step in the combustion of natural gas is:

$$CH_4 + O \longrightarrow CH_3^+ + OH^- \qquad \textbf{2.14}$$

It is further hypothesized that once CH_3 is formed, the remaining major reactions completing combustion to CO_2 and H_2O proceed rapidly. In contrast to methane combustion, hydrogen and air combustion produces hydroxyl radicals rapidly at low

temperatures. The formation of the hydroxyl radicals can help bypass the rate-limiting step by the reaction [17]:

$$CH_4 + OH^- \longrightarrow CH_3^+ + H_2O \qquad \textbf{2.15}$$

The addition of hydrogen to methane increases the number of hydroxyl radicals available to strip the first hydrogen atom from the methane molecule. Bypassing the rate-limiting step causes combustion to occur more rapidly.

This idea was investigated further by Priyadarshi [18] in his master's thesis. By using computer modeling of the entire reaction system, he showed that methane combustion in 30 volume percent HCNG combustion is limited by Eq. 2.16:

$$CH_4 + H^+ \longrightarrow CH_3^+ + H_2 \qquad \textbf{2.16}$$

His findings confirm that the hydroxyl reaction with methane is a rapid reaction. This result suggests that a higher concentration of hydroxyl radicals increases the speed of combustion.

Detailed kinetic modeling in a jet stirred reactor was done by Dagaut et al. [19] using modeling software. The group modeled the kinetics involved in both natural gas–oxygen combustion, and hydrogen-natural gas-oxygen combustion at an equivalence ratio of 0.3. Their study showed that in both cases, methane oxidation is completed via reaction with OH radicals 72 percent of the time. Concurrently, H and O radicals oxidize methane 14 and 10 percent of the time, respectively. With 1.75 percent volumetric addition of hydrogen, the percentage of methane oxidized by OH is unchanged. From this, it can be theorized that OH is the most important reactant in methane oxidation.

Modeling also showed hydrogen addition increases the importance of the reaction below.

$$H + HO_2 \rightarrow OH + OH \qquad \textbf{2.17}$$

Increased activity of Eq. 2.17 [19] increases OH present in the system. The modeled 1.75 percent addition of hydrogen increases the presence of OH radicals by 17 percent. Because of their earlier stated importance to methane combustion, the increased availability of these radicals increases flame propagation.

2.5.4 Experimental Research on HCNG flames

H, O, and OH radicals are of extreme importance in propagating the combustion reaction. The increase in radical formation seen in modeling has also been observed experimentally. Schefer [20] characterized flame structure using OH planar laser-induced fluorescence. A comparison of natural gas flame and 20 percent hydrogen and natural gas flame on a burner produced the graph in Figure **2-4**. The figure shows that increased hydrogen in the fuel increases the surface area of the OH radicals in the flame, allowing more air-fuel mixture to oxidize. The increase in OH concentration in the outer flame was 20 percent. OH radicals reduced 20 percent in concentration in the inner flame. The increased radical availability increases the flame stability, allowing it to run at leaner conditions.

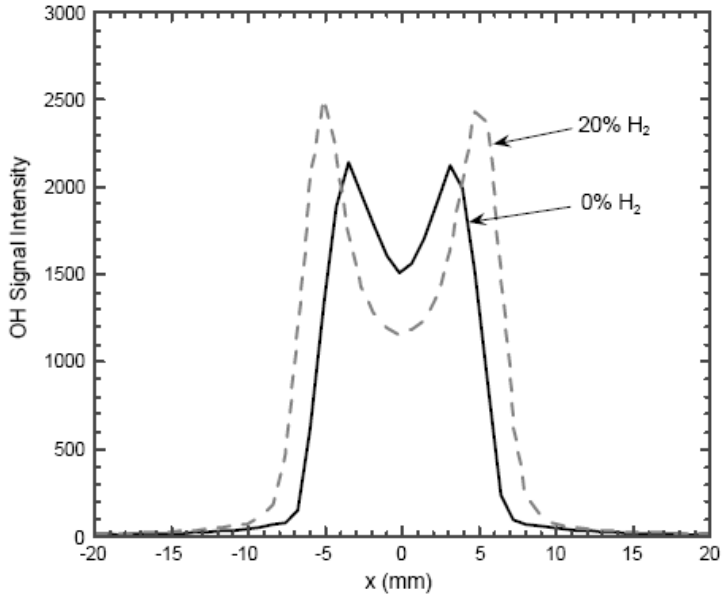

Figure **2-5**: OH Signal Intensity in Natural Gas and 20 Percent HCNG[20]

2.5.5 Spark Timing Adjustments for Optimization

While HCNG mixtures offer an advantage of combustion over CNG, fuels cannot simply be interchanged to obtain optimal efficiency. Researchers have blamed poor performance of HCNG on their failure to reprogram fuel and spark timing maps designed to optimize natural gas utilization in the engine [21].

Nagalingam et al. [22] showed that faster-burning hydrogen produces optimum torque an average of 20 crank angle degrees before that of natural gas. They also reported retardation in optimal spark advance with HCNG due to faster combustion in a research engine running at 1200 rpm. At this point, peak engine power could no longer reach the same level as with natural gas alone. Later research by Collier et al. [23] showed that optimal spark timing reduces from 40 degrees before top dead center (BTDC) to 36

degrees BTDC when hydrogen is added to methane. Reduced combustion duration requires retarded ignition timing to optimize engine output.

2.6 Emissions

Government-mandated emissions regulations are becoming increasingly stringent worldwide. Emissions levels of vehicles used on the road today already require high-cost, complex technology to maintain current emission regulations. To meet the stricter emissions regulations of the future, hydrogen addition is another option for vehicle manufacturers.

Environmentally harmful emissions measured in this study were nitrogen oxide (NO), nitrogen dioxide (NO_2), and carbon monoxide (CO). By changing the fuel composition in the cylinder, some pathways of formation will increase, while others decrease. This section explores how these emissions are formed.

2.6.1 Oxides of Nitrogen

The principal source of nitrogen in nitrogenous oxides (NO, NO_2) is air. It is generally accepted in the scientific community that for stoichiometric air-fuel mixtures, the Zeldovich mechanism governs the production of nitrogen oxide. NO is formed in the flame and postflame gases. The engine compression stroke compresses the burned gases released during the early stages of combustion, increasing their temperature. This temperature increase drives the mechanism to form more NO.

NO_2 is produced in much smaller quantities than NO during normal combustion. It is formed when NO reacts with a hydroperoxyl radical to form a hydroxyl radical and NO_2. More prevalent in light-load diesel combustion, NO_2 is formed when it mixes with cooler fluid, preventing the conversion of NO_2 to NO. In a spark-ignition engine, NO_2 is highest in concentration in a slightly fuel-rich mixture. [11]

2.6.2 CO Formation

Carbon monoxide (CO) emissions are a result of incomplete oxidation. The amount of CO emitted increases with a reduction of excess fuel. CO formation can be summarized by the following reaction [11], in which the R group is the rest of the hydrocarbon.

$$RH \rightarrow R \rightarrow RO_2 \rightarrow RCHO \rightarrow RCO \rightarrow CO \qquad \textbf{2.18}$$

The CO is then converted into CO_2 through the slower reaction of CO and an OH radical.

$$CO + OH \rightarrow CO_2 + H \qquad \textbf{2.19}$$

It is generally accepted that at peak cylinder temperature, the carbon-oxygen-hydrogen system is equilibrated. As the combustion gases cool, the temperature and pressure gradients within the gas cause uneven CO oxidation, resulting in CO emissions [11].

2.6.3 Unburned Hydrocarbons

Hydrocarbon emissions are the consequence of the incomplete combustion of hydrocarbon fuel. While methane in the exhaust is not a regulated hydrocarbon because

of its inert characteristics, pyrolysis and synthesis of methane that occurs during combustion forms other harmful gasses. The resulting oxygenates, carbonyls, and aldehydes contribute to pollution. Unburned hydrocarbons are formed when they are not exposed to the flame front to allow the oxidation reaction to occur. They can be found in crevices on the surface of the cylinder or blow by piston rings, only to reappear in the cylinder after combustion has completed [11].

2.7 HCNG in Test Cell Engines

This study is an attempt to bridge the gap between HCNG test cell research and vehicle testing by determining what happens inside the cylinder during vehicle driving conditions. This section will detail the results researchers obtained using constant speed and load testing on an engine test stand. The following section will review issues related to real driving conditions and look at hydrogen-natural gas testing in the literature. The results will explore correlations between the two.

2.7.1 Part Load Condition HCNG

Spark-ignited engines require a constantly adjusted amount of fuel, proportional to the energy required by the engine to produce the required power output. The throttle valve restricts air coming through the intake to maintain the correct stoichiometry of the air-fuel mixture. Light-load conditions are plagued by incomplete combustion, which decreases thermal efficiency and increases emissions. These conditions compose a large portion of the Federal Driving Cycle [4], which is representative of normal vehicle

operation. Therefore, it is of utmost importance for the vehicle to perform effectively at these conditions.

Engines running at low speed and loads have been found to have slower flame speeds than those running at wide-open throttle. Light-load conditions result in an increased burn time in the cylinder because of lower turbulence. But the slower combustion speed is also a result of a higher concentration of residuals remaining in the cylinder. Such conditions increase the severity of flame initiation and propagation problems.

In order to investigate the relationship between load and burn time, low road loads were tested, by Cattelan et al. [5],who evaluated the brake-specific energy consumption (BSEC) as a function of engine load for Hythane and natural gas. At low loads of 5 and 30 N-m, benefit from the addition of hydrogen was indicated by a decrease in specific energy consumption (BSEC). However, at loads greater than 30 N-m, the difference in BSEC became negligible.

Testing was done on a closed-loop, three-way catalyst engine that controlled the equivalence ratio to 1.0 by Swain et al. [4]. At an equivalence ratio of 1.0, there was only a rise in NO formation from 4.5 to 5.5 g/hp-hr. The smaller increase is BSNOx was attributed to the 4 percent to 5 percent increase in thermal efficiency. Higher loads attenuated thermal efficiency gains when less exhaust gas remained in the cylinder. A reduction in BSCO and BSHC was also observed at low load stoichiometric conditions.

2.7.2 Swirl Addition to HCNG

Swirl is an effective technique to increase mixing of the air-fuel mixture which improves combustion performance. At wide-open throttle conditions, throttling losses are reduced. Other important factors like in-cylinder flow velocity become a more important factor in combustion progress. Using a natural gas engine with hydrogen blends of 0 to 20 percent, Andersson [15] analyzed the difference in combustion between different induced flow velocities. Using the more turbulence inducing quartette head, he found there was no benefit from hydrogen addition.

Stoichiometric combustion of natural gas with hydrogen addition in a high swirl case showed no reduction in ignition delay. At the same conditions with high turbulence, combustion duration did not reduce with addition of hydrogen. The author concluded that during periods of high turbulence the other engine conditions could assist combustion, negating benefits of hydrogen addition.

2.7.3 Hydrogen-Natural Gas Studies

Using cylinder pressure data, Swain et al. [4] tested methane and Hythane burn durations at lean conditions using computer modeling. Two graphs from their results show distinctly different trends. While the testing is only done only for equivalence ratios from 0.65 to 0.80, extrapolated data project the effects of hydrogen at stoichiometric conditions. At stoichiometric conditions, the measure of combustion duration in crank angle degrees converges, indicating that hydrogen has no benefit on stoichiometric methane combustion at 1000 rpm, 1 bar BMEP. However, HCNG and CNG show linear,

parallel trends in flame development angle over the measured equivalence ratios. This indicates that at an equivalence ratio of 1.0, hydrogen reduces the flame development angle.

Karim et al. [24] increased the amount of hydrogen in natural gas and subsequently derived relevant combustion statistics for a variety of equivalence ratios. Hydrogen increased the peak pressure in each cylinder 1 bar for every 10 percent volume hydrogen added. By increasing the concentration of hydrogen in the fuel mixture, a reduction in the length of ignition delay and combustion duration was observed. These results reflect the speeding up of both flame initiation and propagation rates.

2.7.4 Emissions Testing

The latter part of the study will compare emissions data from stationary engine testing and vehicle testing.

Stationary engine testing with producer gas addition, a 33 percent blend of hydrogen with inert gases, was performed by Jensen et al. [25]. Their research explored the change in combustion performance when producer gas was added to natural gas. A statistically significant drop in unburned hydrocarbons was detected. It was determined that combustion enhancement is caused by post oxidation, which is less sensitive to cyclic variations. The lower level of unburned hydrocarbons suggests a more complete combustion, which can be attributed to the faster burning rate of hydrogen. In this instance, hydrogen seems to be a dominating factor in the consumption of hydrocarbons, despite the addition of inert gases as the remaining components in the producer gas like

CO_2, and $N_{2,}$ which retard flame propagation. The reduction in unburned hydrocarbons suggests a more complete combustion of the fuel in the cylinder.

NO emissions increase when hydrogen is added to the natural gas mixture at the same operating air-fuel ratio because hydrogen drives the flame temperature higher. Collier at al. [23] studied the untreated emissions leaving the HCNG engine. NO emissions increased 5 percent at stoichiometric conditions. However when ignition timing was retarded in a lean burn engine with 70:30 HCNG mixture, NOx emissions were controlled to low levels over a range of speed and loads. The spark timing maps on the ECU were installed by Collier technologies that retard spark timing in efforts to reduce NO production from the hotter burning HCNG. More information regarding emissions data across hydrogen-natural gas blends in engine combustion can be found in Akansu's work [10].

2.8 Hydrogen Addition in On-Road Performance

It is impossible for engine manufacturers to predict all the conditions an engine will experience during its lifetime and so engine settings are based on testing done on isolated engine test stands. In these tests, the electronic control unit (ECU) controls engine parameters such as spark ignition, air intake, and fuel injection using data such as temperatures and exhaust composition to optimize engine performance. However, with varying external conditions that occur when the vehicle is on the road, engine loads will fluctuate unpredictably, and the engine can experience in-cylinder combustion variations from cycle to cycle that reduce indicated thermal efficiency. In this final section, issues

related to vehicle performance are reviewed. Next, the background of pressure sensors is explored followed by fundamentals of engine loading.

2.8.1 Vehicle Operating Conditions

Current government standards require engine and vehicle manufacturers to meet specific requirements, which have become more stringent over time. Catalytic converters were first used in commercial gasoline vehicles in 1975 as a way to help meet the mandated emissions requirements. Three different reactions take place in the standard catalytic converter. Two are the oxidation reactions in which unburned hydrocarbons and carbon monoxide are converted to carbon dioxide. A third reaction reduces NO using a platinum-based catalyst to reduce NO to N_2 and O_2.

To catalytically convert these emissions effectively, three-way catalytic converters require that the engine run at stoichiometric conditions. If the fuel mixture is too lean, the oxidation reactions are favored; if it is too rich, the reduction reactions are favored. These results have been shown by Pede et al. [26] in testing on a lean burn HCNG vehicle running the New European Drive Cycle (NEDC). They found that lean operating conditions resulted in higher concentrations of harmful exhaust emissions such as NOx, CO, and UHC's than would be expected under stoichiometric conditions. The different mole fractions inhibit the formation of N_2 and CO_2 in the catalytic converters, minimizing the effect of the lean burn.

2.8.2 Pressure Sensors in Vehicles

While there are few published studies studying heat release through pressure sensors on an actual vehicle, pressure signals do provide important information that can be processed to optimize thermal conversion efficiency. Detection of knock and combustion conditions from the pressure data allows the ECU to finely tune individual cylinder parameters.

A majority of engines on production vehicles are closed loop systems that determine the amount of fuel and air required in the cylinder to produce the appropriate amount of power at the smallest cost to fuel economy and emissions. In the closed loop system, temperature and exhaust information is fed back via the oxygen sensor and thermocouples, and the ECU uses a pre-determined engine map to determine appropriate engine settings. However, exhaust temperature and oxygen content are inaccurate measures of combustion performance. Cylinder pressure sensors give the ECU a better picture of the quality of combustion inside the cylinder. Because the cost of pressure sensors can run into the thousands of dollars, resulting benefits in combustion performance do not justify their use in mass produced vehicles as yet.

Over the past 20 years, in-cylinder pressure sensors have dramatically reduced in cost. To further improve performance and efficiency, engineers have looked at ways to use data for real-time cylinder pressure. Rather than determining combustion performance through sensors external to the combustion process, engineers can look at the signature of combustion through the pressure trace. Using in-cylinder pressure measurements as a feedback sensor, in the place of an oxygen sensor, to control the amount of EGR and the air-fuel ratio is the latest in numerous attempts of engine control

[27]. With the development of more accurate combustion prediction, increased fuel economy and decreased emissions have been achieved. For instance, it is possible to operate the engine at minimum spark advance in order to create conditions for maximum brake torque (MBT), thereby compensating for burn rate and spark requirement differences between cylinders. Cylinder-pressure based control can be adapted for environmental factors, manufacturing variations, component wear, and degradation of various types.

Having a pressure sensor located in the cylinder of a vehicle has been shown to allow a variety of improvements in the vehicle's combustion performance. In the mid-1970s, Hubbard et al. [28] were able to achieve brake-mean effective pressure and fuel economy within 0.1 percent of the theoretical optimum. The pressure sensor in the cylinder enabled the ECU to better understand the combustion in the cylinder. The current study will produce high quality combustion analysis using pressure sensor data.

2.8.3 Vehicle Loads

Propelling a vehicle forward requires the engine to provide energy to the wheels overcoming the load applied from the vehicle surroundings. The instantaneous motion resistance power (P_v) that a vehicle has to overcome to travel at a given speed is a function of speed (v), rolling resistance (R_r), grade resistance (R_g), aerodynamic resistance (R_a) and inertial forces in the vehicle ($\gamma_m$ma). It can be modeled using the following equation [29]:

$$P_v = v(R_r + R_g + R_a + \gamma_m ma) \qquad \textbf{2.20}$$

Other factors that reduce the power available from the engine are accessories loads (P_{ac}) such as air conditioning or interior lighting. Transmission efficiency (η_{tr}) is the energy that will be lost through the transmission. The power equation then becomes [29]:

$$\eta_{tr}(P - P_{ac}) = (R_r + R_g + R_a + \gamma_m ma) \qquad \textbf{2.21}$$

The vehicle powertrain transfers power from the crankshaft in the engine to the wheels. This system includes the transmission, driveshaft, differential, and the final drive. Losses that occur among these interlocking elements are due to vibration, friction, and rotation.

2.8.4 HCNG Vehicle Literature

In order to verify that the engine tests performed in a lab applied to actual testing conditions, Pede et al. [26] tested a 3500 kg truck powered by a 2.8L natural gas engine. Fuel economy and emissions that occurred using HCNG blends of 0, 10, and 15 percent were compared. Primary studies were done on stoichiometric combustion in efforts to reduce tailpipe NOx emissions.

It was found that at the same conditions, retarding the spark timing reduced the levels of NOx dramatically without significantly reducing the output of the engine. In all stoichiometric test cases, the HCNG blends showed reductions in tailpipe hydrocarbons, NOx, and CO_2, when compared to natural gas. The amount of CO emissions decreased with 10 percent hydrogen added, yet increased with 15 percent added. There was a positive linear correlation between fuel economy and quantity of hydrogen. Indicated

thermal efficiency followed a positive linear correlation with hydrogen addition and increased 5 percent with the 15 percent HCNG blend.

Don Karner et al. [21] studied a Dodge Ram Wagon to evaluate fuel and emissions with CNG and HCNG fueling during actual and simulated driving conditions. While in service running on compressed natural gas, the vehicle fuel economy was 13.2 miles-per-gas gallon equivalent (gge). When running on a 15 percent HCNG blend, the same vehicle ran at a more efficient fuel economy of 14.7 miles per gge. When the vehicle was run on the FTP-75 road test, reductions in unburned hydrocarbons, carbon monoxide, and carbon dioxide were seen. A 90 percent increase in NOx was attributed to the fact that the engine was not tuned to optimize HCNG conditions.

While the current study does not focus on emissions, the decrease in fuel economy and increase in NOx emissions should not be as severe because the ECU has been reprogrammed to optimize for HCNG combustion.

Chapter 3

Experimental Set-up

3.1 Outline

The following section begins with an explanation of the engine modification and set-up required for this study. Next, hardware modifications required for this study and the testing procedure are explained. Then the data acquisition system and data analysis methods are discussed. Finally, the engine testing plan is introduced.

3.2 Test Engine and Fueling

In 2004, the Pennsylvania State University purchased a number of fleet vehicles to provide mobility for employees at the Office of the Physical Plant. As part of an initiative to use alternative fuels, Penn State's order included a number of natural gas vans. The vehicle involved in this study is one of those compressed natural gas (CNG) dedicated vehicles, a 2004 Ford E-Series E-250 Van. The stock vehicle meets the van wagon SULEVII emissions standards. Its fuel economy is 18.5 miles per gas gallon equivalent (gge), and it has a range of 280 mi, based on a slow fueling of the tank to 3600 psi [30]. Detailed engine specifications are listed in Table **3-1**.

Table **3-2**: Test Engine Specifications

Engine	SOHC 5.4-Liter, V8, Natural Gas Engine
Displacement	5.4 L
Bore	90 mm
Stroke	106 mm
Compression Ratio	11.0
Connecting Rod Length	169.1 mm
Rated Power	194 kW @ 4500 rpm
Peak Torque	474 Nm @ 2500 rpm
Injection System	Electronically controlled common-rail injection system
Valve Train	2 valves/cylinder

Air Products and Chemicals, Inc. installed a hydrogen fueling station on campus in December of 2005 that dispenses neat hydrogen and HCNG. Together with Collier Technologies, the Pennsylvania State University has developed hydrogen-blend HCNG vehicles on campus to use this station. In these vehicles, Collier Technologies reprogrammed the fuel and spark maps to optimize burning of HCNG, and, to increase power output in the engine, added an Eaton M90 supercharger. A Dynetek carbon fiber reinforced aluminum tank replaced the stock stainless steel fuel tank which is susceptible to hydrogen embrittlement. To allow for switching fuels, interchangeable CNG and HCNG nozzles have been mounted to the fuel port on the side of the vehicle. Fueling is done just like a typical gasoline or diesel pump.

3.3 Engine Instrumentation and Data Acquisition System

While running the vehicle, data were collected on a Dell Dimension desktop computer with a National Instruments PCI-MIO-16E-4 data acquisition card, which has a 333 kilo-samples per second maximum sampling rate. The board reads three signals: a pulse signal every 0.1 crank-angle degree, a pulse signal every 360 crank-angle degrees from the crank angle encoder, and a voltage signal returned from the transducer. The three signals were processed through a data acquisition program written in LabVIEW 7.1 and recorded to a data file.

The piston position and speed were measured using a Model 725 Accu-Coder optical shaft encoder. Every 0.1 change in crank angle degree, a pulse signal was sent to the computer and a cylinder pressure value was recorded. The crank angle encoder was connected to the crankshaft pulley by a custom-made mounting bracket. A grooved aluminum adaptor was bolted inside the crankshaft pulley and attached to a belt that drove the crank angle encoder. Figure **3-1** shows the crank angle encoder set-up mounted on the engine.

A second signal referenced the position of the piston by sending a pulse every 360-degree rotation. Top dead center was determined by using an indicator suspended above the cylinder. This point was confirmed by marking 20 degrees before and after top dead center on the crankshaft adapter at the halfway point. This position was marked on the crankshaft adapter using a scribe. The referencing signal was set to pulse when the piston reached this mark.

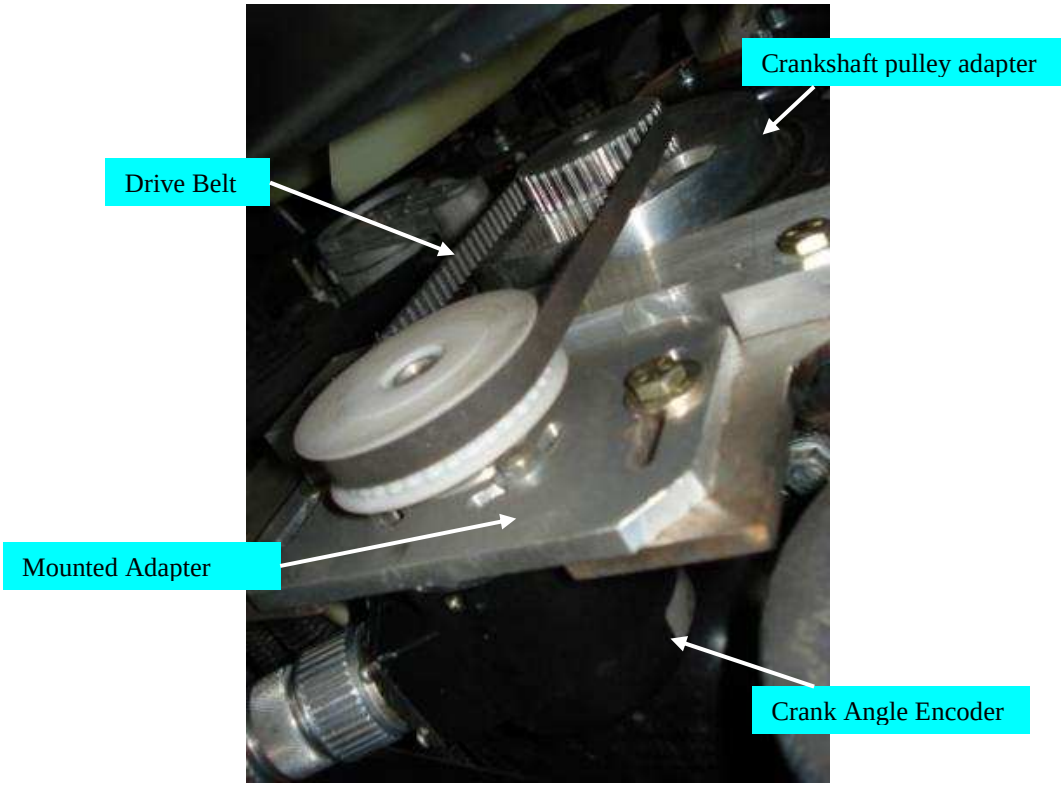

Figure **3-1**: Crankshaft Pulley Adapter to Crank Angle Encoder

Pressure signal measurements were performed using a Kistler Type 6117BCD27 measurement spark plug with an integrated pressure transducer. The working spark plug was removed from cylinder 7 and the Kistler spark plug was inserted in its place. The crystal in the transducer creates an electric charge in picocoulombs as a function of in-cylinder pressure. This charge is passed through a Kistler 5010B charge amplifier, which generates a proportional voltage. The voltage value is recorded using the data acquisition system. Set-up of the pressure transducer system is shown in Figure **3-2**.

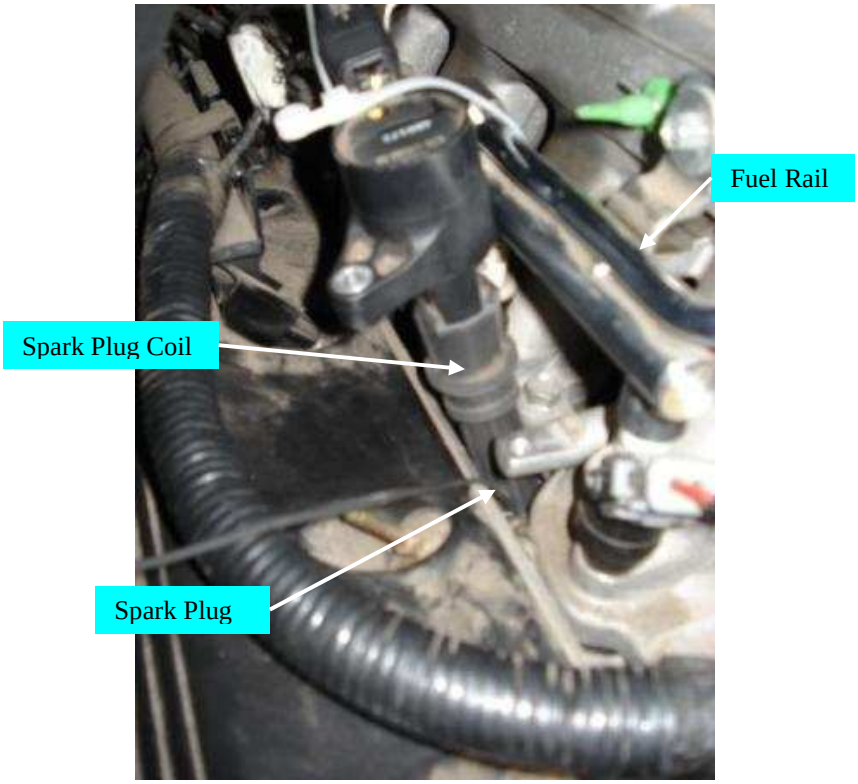

Figure **3-2**: Pressure Transducer Set-Up

In order to obtain steady-state engine conditions, the van was operated on a Clayton Industries model VVT chassis dynamometer, which absorbs energy through large rollers on either side of the rear wheels. These rollers are vehicle-speed limited, and load is controlled by the operator. Testing procedures were set by a test matrix to determine combustion performance at controlled speed and load conditions. Standard driving cycles such as the Federal Transit Protocol (FTP) cycle, etc., were not followed since during such transient test cycles variable pressure conditions occur during combustion preventing steady-state combustion analysis. Instead, stead speed and load conditions were used as the basis for the test procedure. Once the vehicle reaches the pre-

set speed, a driver applied the throttle further with his or her foot to maintain the road load setting. Load conditions are specified in the test matrix.

During testing, engine settings were recorded from the ECU using a scan tool. A series of cables were attached to a laptop running Ford Integrated Diagnostic System (IDS) software, which allowed the user to select individual parameters to read from the engine. Real-time intake air flow and temperature, throttle position, and spark advance were recorded during the test period.

3.4 Fuel Analysis

A gas chromatograph (GC) was used to determine the composition of the two test fuels [31]. Because the gas used in the vehicle could not be sampled readily from the vehicles fuel tank or during the fueling procedure, natural gas was sampled over multiple days and the data averaged to determine the average compositions of the natural gas and the hydrogen-natural gas mixture.

The procedure used to determine fuel composition was as follows: Gaseous fuel was collected in a gas sample bag. A 50-microliter fuel sample was extracted with a syringe, and injected into the GC. The sample port volume was 1mL, made up of the 50 microliter sample along with 950 microliters of argon (carrier gas). This procedure was executed twice, once for the flame ionization detector (for low molecular weight hydrocarbons), and then for the thermal conductivity detector (for hydrogen and nitrogen).

The gas chromatograph was calibrated for methane, ethylene, ethane, propylene, propane, butylene, butane, and hydrogen, for the ranges typically found in natural gas. The chromatogram provided the mole fraction of each constituent. That mole fraction was then multiplied by 20 to bring the mole fractions up to the 1-microliter basis.

3.5 Semtech-DS Emissions Equipment

Emissions data from the test vehicle were collected externally using a Semtech-DS, which is an onboard emissions testing system produced by Sensors, Inc., Saline, Michigan. The Semtech-DS uses a combination of methods, including Flame Ionization Detection (FID) with Non-Dispersive Infrared (NDIR) and Non-Dispersive Ultraviolet (NDUV). These methods allow for direct comparisons in test cell measurements for THC, CO, CO_2, NO, and NO_2 in compliance with CFR-40, 1065 Subpart J. A distinct advantage of this technology is its ability to absorb high shock or vibration, while providing accuracy, and resolution in a short response time. In these tests, the FID was not operational and no hydrocarbon data were recorded.

The following system was used to obtain exhaust gas for analysis: Immediately after exiting the exhaust manifold, a portion of the exhaust gases passed through a one-quarter-inch hole drilled into the exhaust pipe. A Swagelok weld fitting was attached to the exhaust pipe through which the exhaust sample flowed into a foot-long steel tube designed to protect the heated lines of the emissions analyzer. Exhaust gas continued through to a 190 °C heated line into the Semtech-DS to be analyzed.

Using an exhaust flowmeter linked to the vehicle's on-board computer, the user could instantaneously measure emissions data as a function of engine performance in g/km, g/kg fuel, or g/bhp-hr. In addition, the testing block had communications and global positioning system modules. Data could be provided over cellular or Internet links in addition to on-board collection and storage. Since the vehicle was operated on a chassis dynamometer rather than over the road, this communications technology was not utilized.

The CO, CO_2, O_2, NO, and NO_2 concentrations were recorded on both a wet and dry sample basis. For the purposes of this report, they are reported on a dry sample basis. Table **3-3** is a summary of the measurement techniques used by the Semtech-DS.

Table **3-3**: Summary of Exhaust Species and Measuring Techniques

Measure Gaseous Species (units)	Measurement Technique
CO (volume percent)	NDIR
CO2 (ppm)	NDIR
O2 (volume percent)	Paramagnetic detector
NO (ppm)	NDUV resonant absorption spectroscopy
NO2 (ppm)	NDUV resonant absorption spectroscopy

3.6 Testing Procedure

The testing took place on the chassis dynamometer located adjacent to the Pennsylvania Transportation Institute at University Park, Pennsylvania. The pressure sensor and crank angle encoder were installed and connected to the data acquisition system. Exhaust gas recirculation (EGR) was prevented from entering the intake by disconnecting the EGR control valve connected to the throttle. Finally, it was verified

that the referencing signal from the crank angle encoder was being sent when the piston reached top dead center. The vehicle was prepared to run once the instruments needed to run the experiment and record data were set up.

The engine was then turned on and warmed up until the coolant temperature held a constant reading on the dashboard. Because there was no passive cooling of the engine, a large fan drew fresh air into the laboratory from outside the building. To run the test, the driver applied the throttle to bring the vehicle to the chassis dynamometer limited vehicle speeds of 15 or 30 miles per hour. The driver would then increase throttle position to maintain a road load of 10, 20, or 30 horsepower. At each road load setting, an averaged 200 cycle pressure trace was saved to a file using LabVIEW. Updated scan tool data were read by the emissions system and saved to a separate file.

3.7 Heat Release Analysis

To investigate the effect of hydrogen on natural gas combustion, apparent heat-release rate calculations for both fuels were performed. Heat release rate data allow for comparison of combustion performance for the two fuels. In this study a zero-dimensional single zone model for the apparent heat release rate calculation [11] was used. This model is based on the following assumptions. First, the mixture is distributed homogeneously and has uniform properties throughout the cylinder. Second, the calculated ratio of specific heats of the in-cylinder gas mixture is assumed to be the same as that of air. Finally, the heat release due to combustion is considered to be heat addition to the cylinder.

The apparent heat release rate was calculated based on the cylinder pressure data using the first law of thermodynamics as described by Heywood [11]. The in-cylinder pressure changes as a result of cylinder volume, combustion, heat transfer effects, flow into crevices, and leakage. The most significant contributors to pressure increase are volume change and combustion.

Heywood defines the chemical heat release rate, or gross heat release rate as shown in Eq. **3.1**. Literally, the gross heat release rate is the "chemical energy" of the fuel that is released by combustion.

$$\partial Q_{ch} = dU_s + \partial Q_{ht} + \partial W + \sum h_i dm_i \qquad \textbf{3.1}$$

The apparent heat release rate, also known as the net heat release rate, is the chemical heat release rate minus the losses incurred by heat transfer to the walls and crevice volume losses, as shown in Eq. **3.2**. Because proper instrumentation to determine blow-by and crevice volume was restricted due to space considerations, the model used assumed heat transfer and crevice effects to be zero.

$$dQ_{ch} = dQ_n - \partial Q_{ht} - \sum h_i dm_i \qquad \textbf{3.2}$$

Net work and sensible energy of the charge determine the apparent heat release rate in Eq. **3.3**. The equation for net heat release that includes measured variables is shown in Eq. **3.4**. Differentiating the ideal gas law gives Eq. **3.5.**

$$\frac{dQ_n}{dt} = \frac{dU_s}{dt} + \frac{dW}{dt} \qquad \textbf{3.3}$$

$$\frac{dQ_n}{dt} = mc_v \frac{dT}{dt} + p\frac{dV}{dt} \qquad \textbf{3.4}$$

$$PdV + VdP = mRdT \qquad \textbf{3.5}$$

Substituting the ideal gas law into Eq. **3.4** gives Eq. **3.6**.

$$\frac{dQ_n}{dt} = (1 + \frac{c_v}{R}) * P\frac{dV}{dt} + \frac{c_v}{R}V\frac{dP}{dT} \qquad \textbf{3.6}$$

The value for the C_v/R term is found using the ratio of specific heats as is found in Heywood as Eq. **3.7,** and will give Eq. **3.8** when substituted into Eq. **3.6**.

$$\frac{c_v}{R} = \frac{1}{\gamma - 1} \qquad \textbf{3.7}$$

$$\frac{dQ_n}{dt} = \frac{\gamma}{\gamma - 1}P\frac{dV}{dt} + \frac{1}{\gamma - 1}V\frac{dP}{dt} \qquad \textbf{3.8}$$

The ratio of specific heats for the mixture is calculated using the equations below. For bulk cylinder temperatures less than 1000 degrees Kelvin, Eq. **3.9** is used. For temperatures greater than 1000 degrees Kelvin, Eq. **3.10** is used [32].

$$\gamma = 1.3 + 6.0*10^{-5}*\mathrm{T} - 1.5*10^{-7}*\mathrm{T}^2 - 5.6*10^{-11}*\mathrm{T}^3 + 9.2*10^{-14}*\mathrm{T}^4 \qquad \textbf{3.9}$$

$$\gamma = 1.4 - 2.5*10^{-4}*\mathrm{T} + 1.4*10^{-7}*\mathrm{T}^2 - 3.7*10^{-11}*\mathrm{T}^3 + 3.7*10^{-15}*\mathrm{T}^4 \qquad \textbf{3.10}$$

Calculation of the bulk cylinder temperature was performed using Eq. **3.11**, rearranged and with respect to crank angle position. The integral in Eq. **3.12** gives the bulk cylinder temperature.

$$\frac{dT}{d\theta} = \frac{1}{(m_{air} + m_{fuel})c_v} * (\frac{dQ_n}{d\theta} - p\frac{dV}{d\theta}) \qquad \textbf{3.11}$$

$$T(\theta_i) = \int \frac{dT}{d\theta} d\theta \qquad \textbf{3.12}$$

In order for heat release calculations to be accurate, pressure data must meet four criteria: First, the correct reference pressure must be used to convert pressure signals to absolute pressures. Second, the pressure versus crank angle degree phasing is accurate to

within 0.2 crank angle degrees. Third, clearance volume is estimated with sufficient accuracy. And finally, transducer temperature variations due to wall heat flux are held to a minimum.

Pressure measurements were averaged over 200 cycles with 0.1 crank angle degree resolution. Figure **3-3** is a 200-cycle average pressure trace of natural gas combustion at a high speed and load.

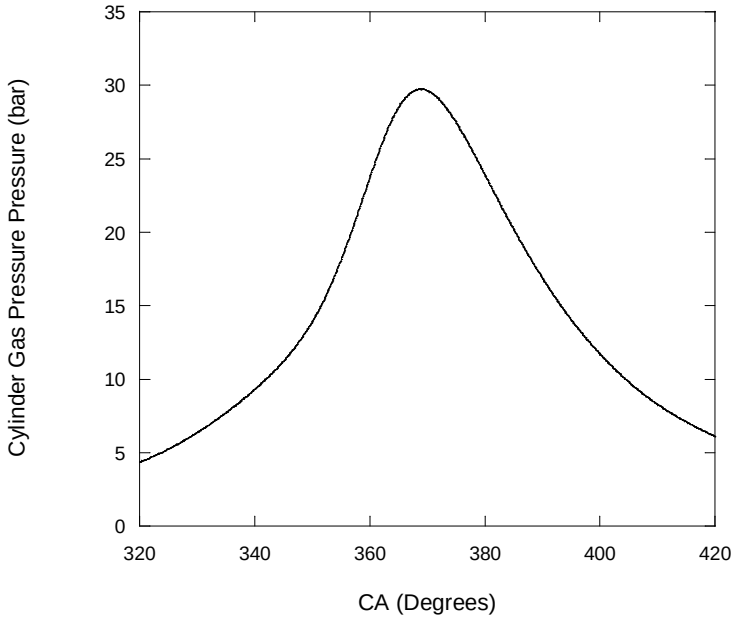

Figure **3-3**: 200 Cycle Averaged Cylinder Pressure Trace

In order to perform the heat release rate calculations, two derivative terms are needed, $dV/d\theta$ and $dP/d\theta$. The derivative of volume can be calculated using the first order central difference scheme shown in Eq. **3.13**. Any noise in the pressure signal can be detrimental to the heat release calculations. This is because the heat release is a derivative of the pressure trace, and any noise will be magnified. To reduce this problem, a fourth

order central finite difference is used to calculate the derivative of pressure, as shown in Eq. **3.14**.

$$\frac{dV_i}{d\theta} = \frac{V_{i+1} - V_{i-1}}{2 * \Delta\theta} \quad \textbf{3.13}$$

$$\frac{dP_i}{d\theta} = \frac{P_{i-2} - 8 * P_{i-2} + 8 * P_{i+1} - P_{i+2}}{12 * \Delta\theta} \quad \textbf{3.14}$$

An example of an instantaneous heat release graph is given in Figure **3-4**.

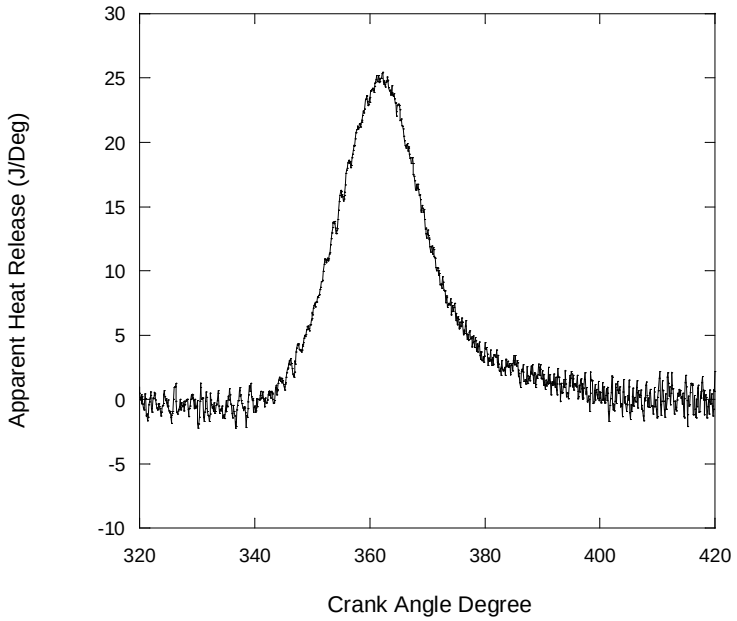

Figure **3-4**: Instantaneous Heat Release Rate

The cumulative heat release is calculated by integrating the apparent heat release rate, as shown in Eq. **3.15**. To determine the mass fraction burned, heat release is converted into a percentage relative to maximum cumulative heat release. For each crank angle degree after the start of combustion, the percentage of maximum cumulative heat release is calculated using Eq. **3.16**. For the purposes of this study, the percentage of heat released is equal to the percentage of mass fraction burned.

$$Q(\theta_i) = \int_{\theta_{soc}}^{\theta_i} \frac{dQ_n}{d\theta} d\theta \quad \textbf{3.15}$$

$$Q\% = \frac{Q_i}{Q_{\max}} \quad \textbf{3.16}$$

3.8 Calculating Air-Fuel Ratio

Heat release calculations require accurate determination of the mass of air and fuel inside the instrumented cylinder. The mass of air in the cylinder is calculated using the air flow rate entering the intake mainfold. Mass of fuel is calculated using the air-fuel ratio determined by emissions data.

The method used to determine air-fuel ratio comes from work by Spindt [33]. In the Spindt method, the air-fuel ratio can be determined from the ratios of the wet exhaust components CO_2, CO, O_2, and unburned hydrocarbons. Because unburned hydrocarbon values were not recorded due to the inoperable FID, they were assumed to be equivalent to the baseline test in Cattelan et al. [5]. The fraction of hydrogen and carbon in the fuel are found using Eq. **3.17** and Eq. **3.18** based on the C_xH_y composition of the fuel.

$$F_c = \frac{12.01 * x}{12.01 * x + 2.016 * y} \quad \textbf{3.17}$$

$$F_h = \frac{2.016 * y}{12.01 * x + 2.016 * y} \quad \textbf{3.18}$$

Ratios of the exhaust products are determined from the mole fractions of O_2, CO_2, CO and HC in Eq. **3.19,** Eq. **3.20** and Eq. **3.21**.

$$Q = \frac{P_{O_2}}{P_{CO_2}} \quad \textbf{3.19}$$

$$R = \frac{P_{CO}}{P_{CO_2}} \quad \textbf{3.20}$$

$$F_b = \frac{P_{CO} + P_{CO_2}}{P_{CO} + P_{CO_2} + P_{HC}} \quad \textbf{3.21}$$

These relationships are used in Eq. **3.22** to determine the approximate air-fuel ratio of the intake charge.

$$(A/F)_{ratio} = F_b(11.492 * F_c(\frac{1+R/2+Q}{1+R}) + (\frac{120 * F_h}{3.5+R})) \quad \textbf{3.22}$$

3.9 Test Plan

The objective of this study was to determine the effects of hydrogen on natural gas combustion under a variety of test conditions in order to determine how hydrogen benefits the efficiency of natural gas combustion in vehicles.

Fuels used in this study were compressed natural gas (CNG) and a 33 percent hydrogen-compressed natural gas (HCNG) blend, with hydrogen representing 9 percent of the energy of the fuel in the HCNG. The natural gas source was the same for each test, and the hydrogen was generated by the Air Products and Chemicals, Inc. fueling station via steam reforming of methane, which was then blended with natural gas. Detailed fuel composition information can be found in Appendix A.

Hydrogen was expected to increase combustion performance at low-speed and load conditions. Each fuel was tested at identical vehicle conditions. Normal operation was tested with the transmission in the “D” position. To evaluate fuel changes at high

engine speeds, the automatic transmission was placed in position D1. Table **3-4** details the test conditions used in investigating the effect of hydrogen on combustion during various driving conditions.

Table **3-4**: Test Matrix

Fuel: CNG

Road Load (horsepower)	10	20	30
Transmission Position	D/D1		
Vehicle Speed (miles/hour)	15/30		

Fuel: HCNG

Road Load (horsepower)	10	20	30
Transmission Position	D/D1		
Vehicle Speed (miles/hour)	15/30		

Chapter 4

Results and Discussion

4.1 Introduction

This chapter is divided into five parts. In the first section, the calculations and data read from the vehicle are evaluated. The second section reviews the measures of combustion performance, including ignition delay, combustion duration, and coefficient of variance, as a function of fuel. In the third part, the effect of engine speed and vehicle load on combustion for both fuels is investigated. Next, emissions performance with hydrogen addition to natural gas is investigated. Finally, how the combustion performance in the cylinder changes as a function of vehicle speed is reviewed.

4.2 Engine and Fuel Conditions

In this section, the fuel and engine conditions necessary for analyzing engine performance were recorded and calculated. The air-fuel ratio was calculated using emissions data. Because of the lack of instrumentation on the vehicle, the air-fuel ratio had to be calculated using raw exhaust data. Spark timing was determined by the electronic control unit, which controls the beginning of combustion in the spark-ignited engine.

4.2.1 Air-Fuel Ratio

The air-fuel ratios for HCNG, which were calculated using the Spindt method, appear in Figure **4-1**. The same method was used to calculate CNG air-fuel ratios, which are given in Figure **4-2**. Because equipment limitations did not provide all variables required to compute air-fuel ratio, stoichiometric hydrocarbon results from Cattelan et al. [5] were used. The error bars on the graph were the result of the 95 percent confidence interval of CO on the air-fuel ratio calculation.

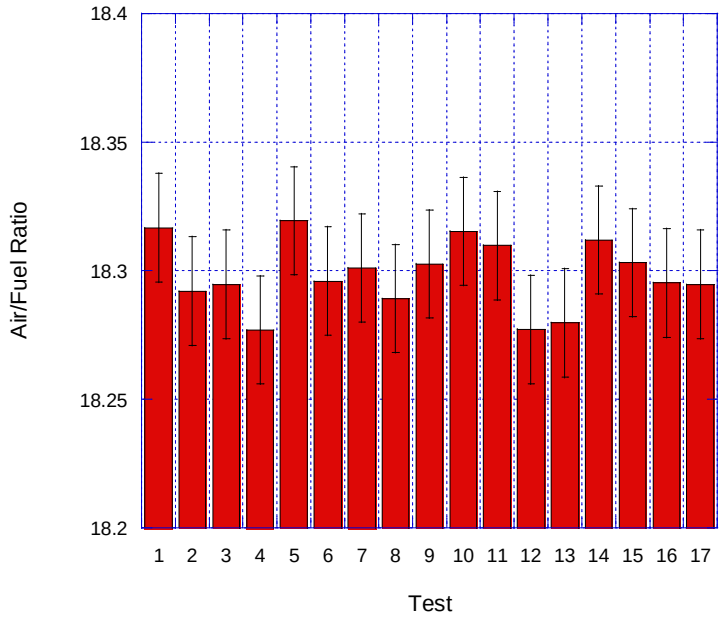

4-1: Air-Fuel Ratio for HCNG testing

The average HCNG air-fuel ratio calculated using the Spindt method is 18.29. Air-fuel ratio values for CNG combustion averaged 17.38. Using the methane and hydrogen components measured in the gas chromatograph, stoichiometric HCNG and CNG combustion with air have air-fuel ratios of 18.10 and 17.18, respectively. These values are close to those in Figure **4-1** and Figure **4-2**, where air-fuel ratios recorded

fluctuations of less than 1 percent. For the purposes of this study, it can be assumed that engine control is fine-tuned to stoichiometric conditions.

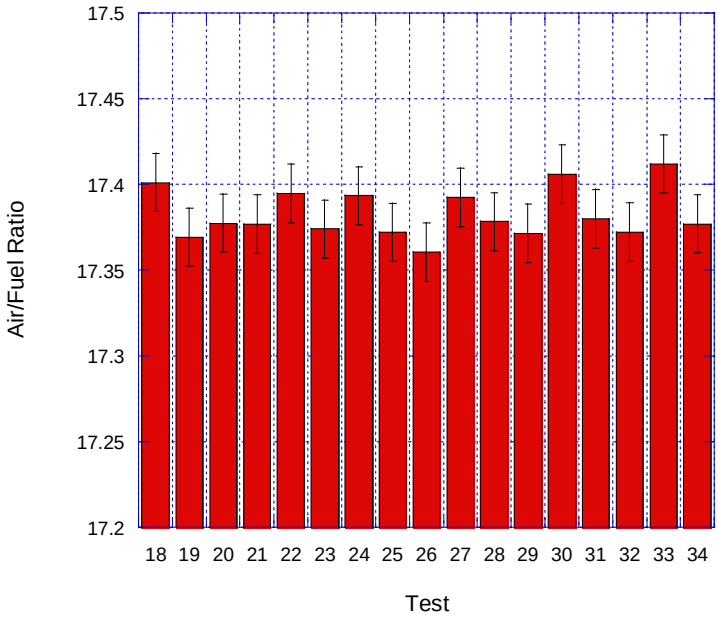

Figure **4-2**: Air-Fuel Ratio for CNG testing

4.2.2 Spark Advance

Spark-ignited engines use an electrically generated charge to begin the combustion process in the cylinder. In the vehicle used in this research, spark timing maps optimized performance by controling the engine to “learn” the most efficienct HCNG spark timing. These map data points were read off of the scan tool during the testing, at vehicle speeds of 15 miles per hour and 30 miles per hour. The average values for spark advance timings using CNG and HCNG are found in Table **4-1.** While there

was some variation in spark advance at the same speed and load, this was probably a result of the highly sensitive nature of the throttle which was difficult to control. This data shows that spark advance is a function of throttle position and unaffected by fuel composition.

Table **4-1**: Spark Advance Timings

Vehicle Speed: 15 MPH

Transmission Position D (low speed)	CNG Spark Advance (BTDC)	HCNG Spark Advance (BTDC)
10 hp	23	23.5
20 hp	22.5	22.5
30 hp	22	22
Transmission Position D1 (high speed)	CNG Spark Advance (BTDC)	HCNG Spark Advance (BTDC)
10 hp	27.5	27.5
20 hp	25	25.5
30 hp	24	24.5

Vehicle Speed: 30 MPH

Transmission Position D (low speed)	CNG Spark Advance (BTDC)	HCNG Spark Advance (BTDC)
10 hp	22.5	22.5
20 hp	20.5	21
30 hp	19.5	19.5
Transmission Position D1 (high speed)	CNG Spark Advance (BTDC)	HCNG Spark Advance (BTDC)
10 hp	32	32.5
20 hp	31	31
30 hp	29.5	30.5

4.3 Characteristics of Hydrogen Combustion

Combustion characterization describes how the air-fuel charge inside the cylinder is burned. In the next section, the effect of 33 percent hydrogen on natural gas combustion in the spark-ignition engine at 1350 RPM, 40 percent wide-open throttle and 1370 RPM, 67 percent wide-open throttle are compared. This section shows the pressure measurements, heat release trends, and combustion duration, as well as temperature and coefficient of variance.

4.3.1 Pressure

Pressure measurements are useful tools for indicating variations in the phasing and duration of combustion. They are also used to calculate the apparent heat release rate.

Under identical speed and load conditions, pressure during combustion of HCNG was greater than that of neat natural gas. Two examples of pressure during a combustion cycle from the 30 miles-per-hour test are found in Figure **4-3** and Figure **4-4**. Karim et al. [24] observed an increase of pressure of 1 bar per 10 percent hydrogen addition during lean burn conditions. In this study, at stoichiometric conditions, a larger increase in peak pressure is seen. A 5 bar increase in peak pressure with HCNG is observed, equivalent to a 1.5 bar increase per 10 percent hydrogen addition.

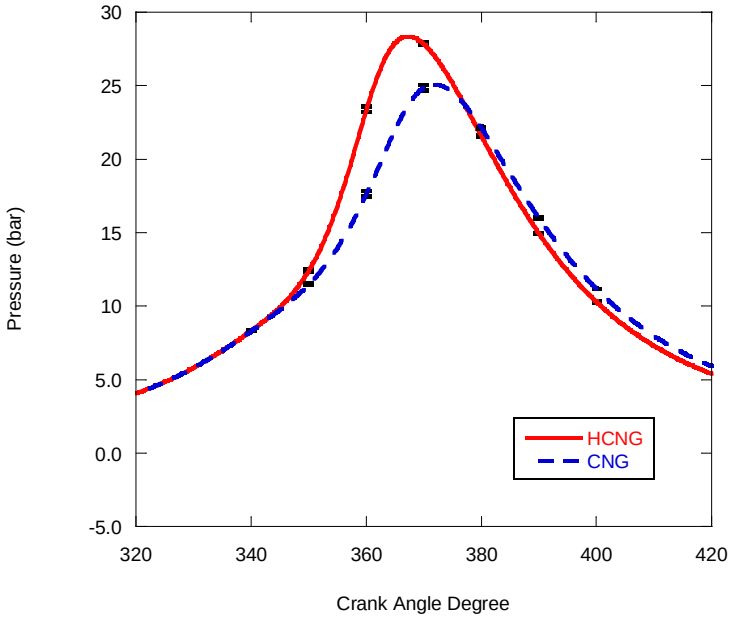

Figure **4-3**: 200 Cycle Averaged Pressure Trace, 1350 RPM, 10 horsepower road load

Volume change and combustion have the largest effects on cylinder pressure [11]. Since there are no volumetric changes in the cylinder, the pressure increases that occur in the cylinder are a result of the HCNG combustion process. As Figure **4-3** and Figure **4-4** show, HCNG increases the pressure at a much more rapid pace than CNG, peaking close to top dead center. Pressure after spark discharge is indicative of heat release of the fuel during combustion. Peak pressure occurring closer to top dead center more closely resembles the Otto cycle, which indicates an increase in the thermal efficiency of the combustion.

Error bars show the 95 percent confidence interval on the pressure data during areas of high uncertainty. Because the pressure is used to calculate the rest of the combustion statistics in this section, it is assumed the characteristics of combustion are statistically significant.

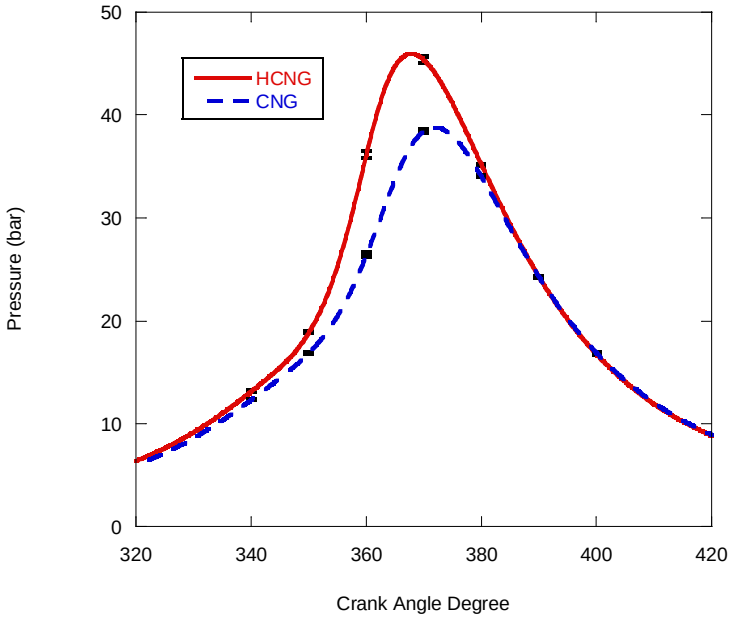

Figure **4-4**: 200 Cycle Averaged Pressure Trace, 1370 RPM, 30 horsepower road load

4.3.2 Apparent Heat Release

To study the effect of fuel on bulk combustion characteristics, heat release analyses were performed at all testing conditions. The heat release rates were different between the two fuels, as shown in Figure **4-5** and Figure **4-6**. These figures showed that hydrogen addition resulted in a faster release of fuel energy, when compared with CNG. The results also indicated that HCNG combustion peak heat release rate increases 25 percent and occurs 9 crank angle degrees before that of CNG.

Increased heat release early in the power stroke puts extra stress on the structural integrity of the cylinder, and increases NO formation, but it also allows for best indicated thermal efficiency. In Figure **4-5** and Figure **4-6** HCNG releases more than half of the

energy during the compression stroke, before top dead center. Energy released when the volume of the cylinder is decreasing works against the motion of the piston decreasing indicated work, which causes a decrease in the power output of the cylinder. These are considerable throttling losses that detract from the thermal efficiency of the combustion process with HCNG.

The heat release characteristics in this study exhibit non-ideal combustion. Heywood [11] states that addition of exhaust gas recirculation (EGR) increases the burn duration in the cylinder. In the case study, EGR of 20 percent increases the flame development angle and combustion duration 50 percent. If the exhaust gas recirculation valve was connected, it would retard heat release, reducing losses in indicated work.

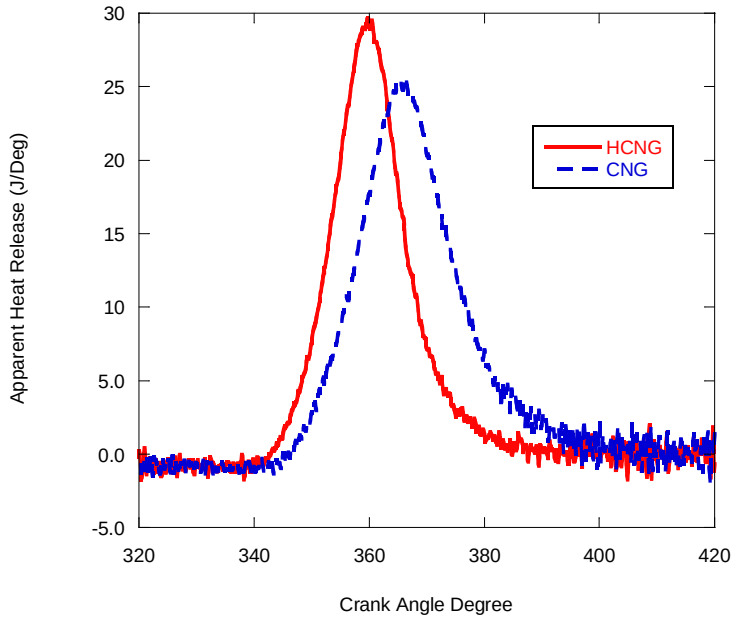

Figure **4-5**: Heat Release Rate 1350 RPM, 10 horsepower Road Load

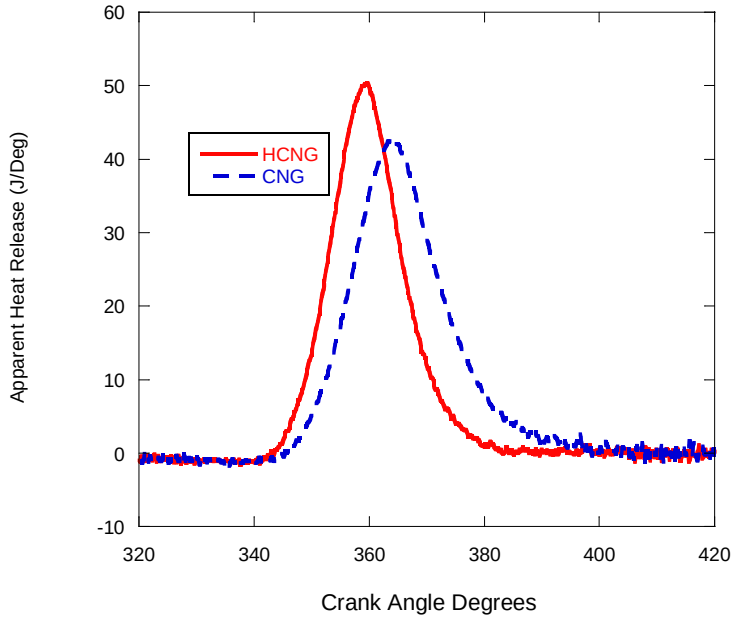

Figure **4-6**: Heat Release Rate 1370 RPM, 30 horsepower Road Load

4.3.2 Fuel Burning Rates

The computed mass fraction burned approximates the burned mass inside the cylinder and are an indicator of combustion performance within the cylinder. Normalized heat release is representative of the mass fraction burned in the cylinder. Figure **4-7** and Figure **4-8** show the normalized cumulative heat release that occurred at 1350 and 1370 RPM, both at 30 hp road load.

It is advantageous to characterize different stages of combustion by the duration in crank angle degrees. The crank angle degrees covered during each stage of combustion are indicative of the combustion process. Figure **4-7** and Figure **4-8** show that compared with natural gas, hydrogen addition decreases the flame development angle and

combustion duration. Hydrogen also causes more fuel to burn before top dead center. This early burn of the fuel releases energy during the compression stroke, which results in a decrease in thermal efficiency.

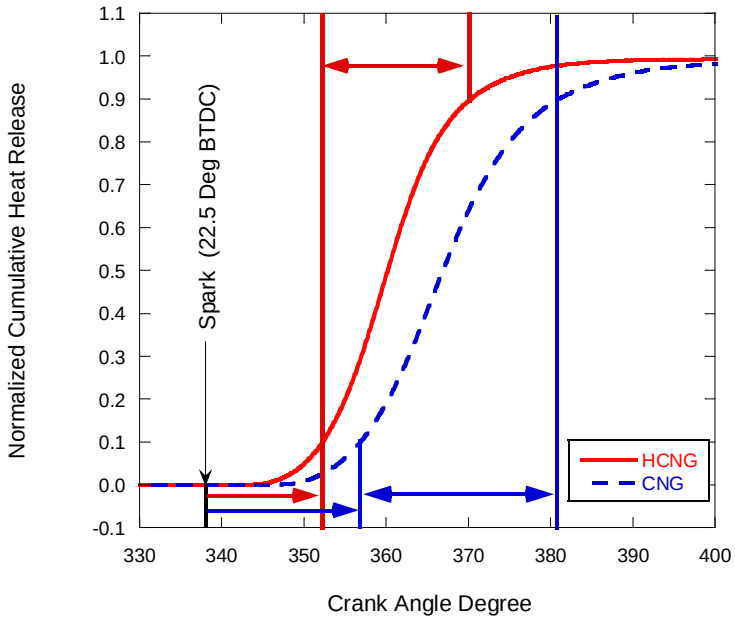

Figure **4-7**: Normalized Heat Release 1350 RPM, 10 hp Road Load

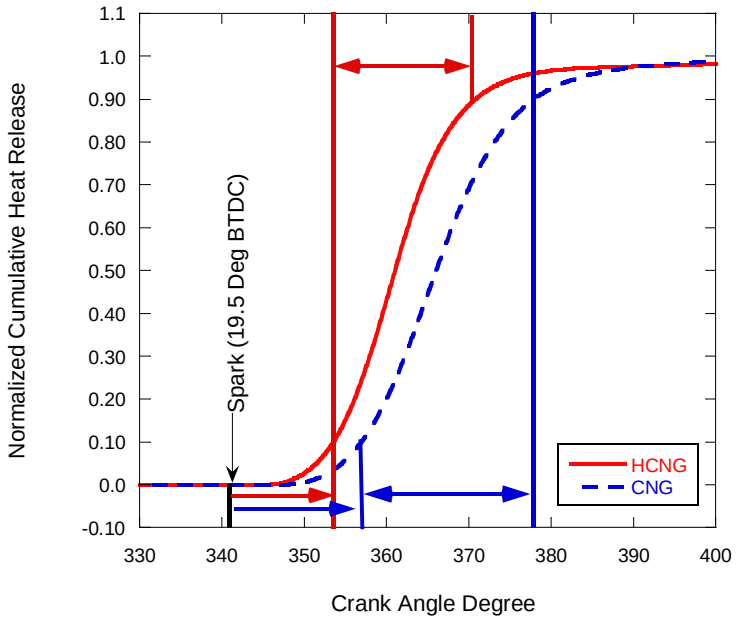

Figure **4-8**: Normalized Heat Release 1370 RPM, 30 hp Road Load

The quicker burn reduces the amount of time during the combustion cycle that the gases are at high temperature, which results in a reduction in heat transfer losses. The slope of the line in Figures **4-7** and Figure **4-8** during the combustion duration is indicative of the speed of the fuel burn. While both fuels begin combustion at the same time, the HCNG combustion reaction progresses much faster.

Figure **4-9** shows the peak heat release rate for the tests run at 30 miles per hour. A higher heat release rate indicates a larger mass of fuel being burned per crank angle degree. As this figure shows, the addition of hydrogen to natural gas increases the peak burn rate of the fuel and is independent of load. At all testing conditions, HCNG increases the maximum burn rate of the fuel by 25 percent, compared with CNG.

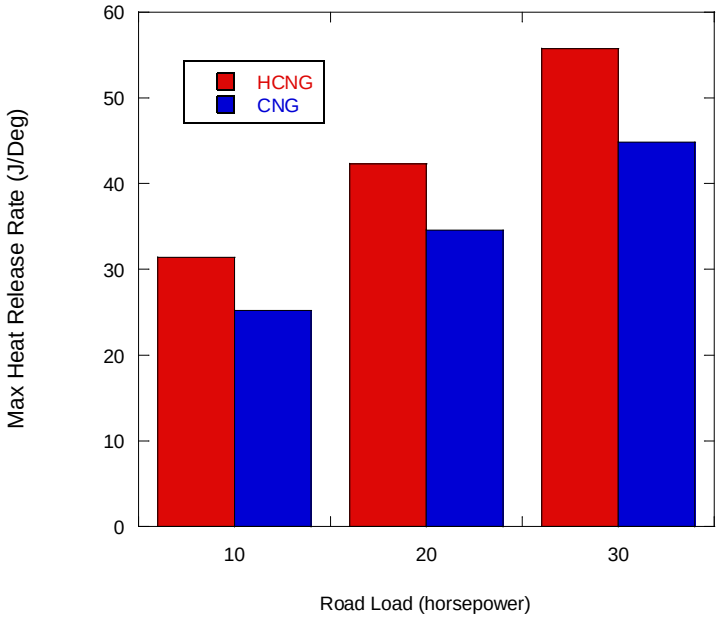

4-9: Peak Heat Release Rate at 1350, 1360 and 1370 RPM, 30 mph

4.3.3 Calculated In-Cylinder Temperature

An increase in bulk cylinder temperature contributes to heat loss to the surroundings and drives NO formation. The temperatures calculated using the pressure data show that the rapid combustion of HCNG increase the bulk cylinder temperature.

In this study, an increase in temperatures from 7 to 10 percent was observed with hydrogen addition. Figure **4-10** and Figure **4-11** show the single-zone analysis of bulk cylinder temperature at 1350 and 1370 RPM. It must be noted that during normal operation, the vehicle as modified by Collier Technologies employed a significant amount of supplemental exhaust gas recirculation in order to lower combustion temperatures and prevent NOx formation.

The peak temperature for HCNG combustion occurs closer to top dead center, when the volume of the cylinder is the smallest. Intense heat at this stage in combustion increases the transfer of heat to the combustion chamber surfaces, which reduces the pressure of the system. Increased temperature is sustained across a longer period during HCNG combustion than with CNG. The more time HCNG spends at high temperature, the more NO formation occurs.

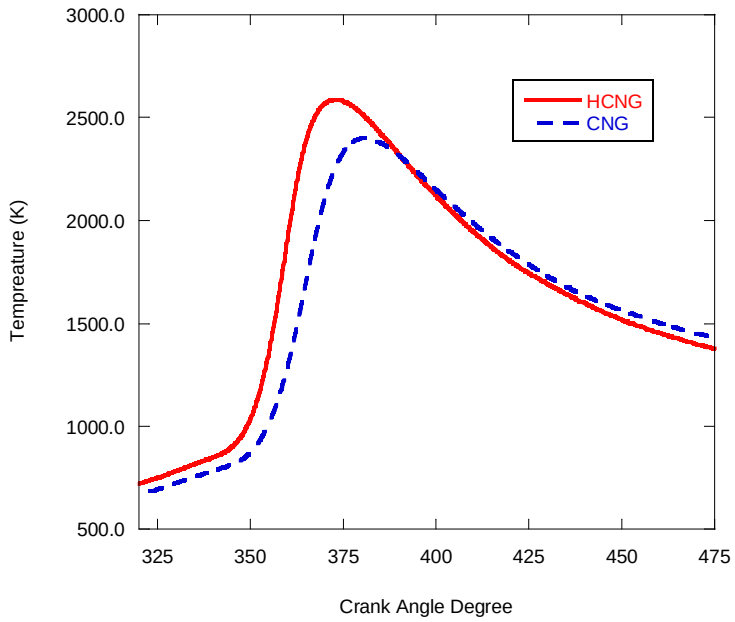

Figure **4-10**: Bulk Cylinder Temperature 1350 RPM, 10 hp Road Load

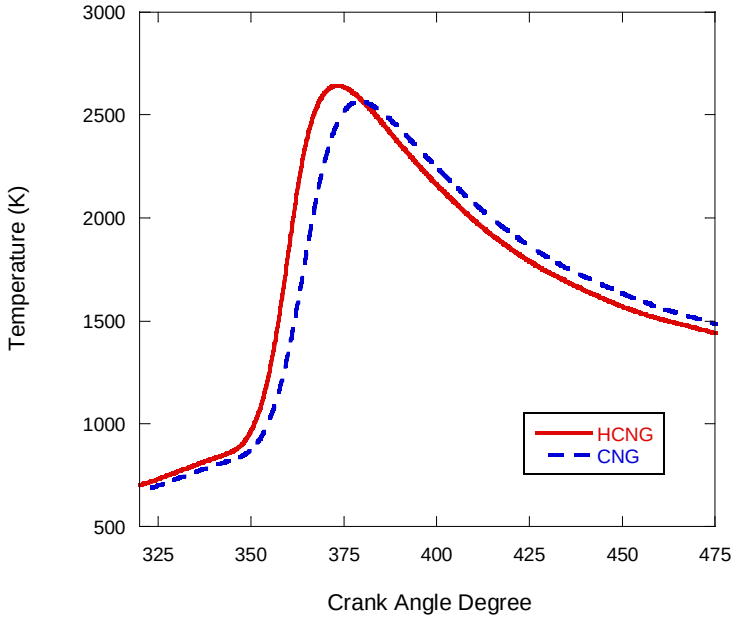

4-11: Bulk Cylinder Temperature 1370 RPM, 30 hp Road Load

4.3.4 Heat Transfer

Reducing the heat loss to the surroundings can increase the thermal efficiency of combustion. Previous findings [1] have attributed increased thermal efficiency in HCNG combustion, when compared to CNG combustion, to a faster burn time. This increased efficiency with HCNG occurs because lower combustion duration reduces the time for which the cylinder is at high temperatures, losing heat to the surroundings. In this study, the amount of heat lost to the outer walls and carried away by the coolant was calculated using the Woschni heat transfer correlation.

The expansion stroke is where the most significant heat transfer losses occur. There, the heat transfer will cause the gas pressure in the cycle to fall below isentropic

expansion as the volume increases, resulting in a decrease in thermal efficiency. Figure **4-12** and Figure **4-13** show the Neat Heat Release and Heat Transfer at 1350 and 1370 RPM. The figures indicate the cumulative heat transferred as net work on the system, Qn, and heat transferred to the surroundings, Qht.

More heat is transferred to the surroundings because of elevated combustion temperatures with HCNG combustion. While previous published work has stated that HCNG's decrease in combustion duration would reduce the heat transfer to the surroundings, an earlier start of combustion and higher bulk cylinder temperatures result in greater transfer of energy to the cylinder wall.

It is interesting to note that as much as 50 percent of the energy available in the cylinder is lost to the coolant. While this number appears to be high, low speed and load conditions for a six-cylinder spark-ignited engine at the same engine speed were found by Ament et al. [34] to lose 50 percent of the fuel heating value to the coolant load. This validates the high heat transfer rates for HCNG and CNG combustion found in this study.

Net heat release is equal to the sensible energy change and work transfer to the piston [11]. Since these two traces are run at the same operating conditions, it can be assumed that the work transferred to the piston is equal. Neat natural gas combustion has a higher net heat release than HCNG because of the increased losses via heat transfer to the surroundings.

As the engine load increases, the difference in energy losses between the HCNG and CNG is reduced. As the engine load increases, a higher percentage of fuel energy is converted to work on the piston, with only 40 percent of energy lost to the surroundings.

During the increase engine load, combustion is more complete which reduces the impact of the hydrogen.

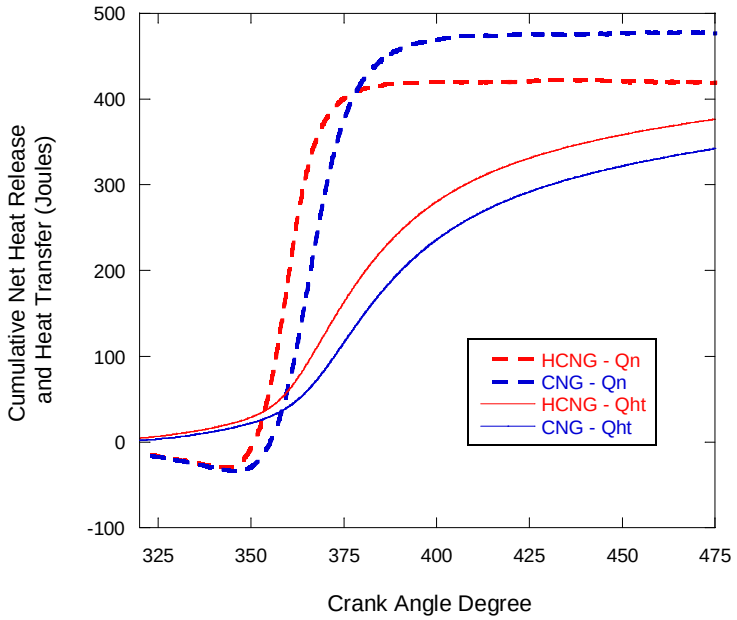

Figure **4-12**: Neat Heat Release and Heat Transfer 1350 RPM, 10 hp Road Load

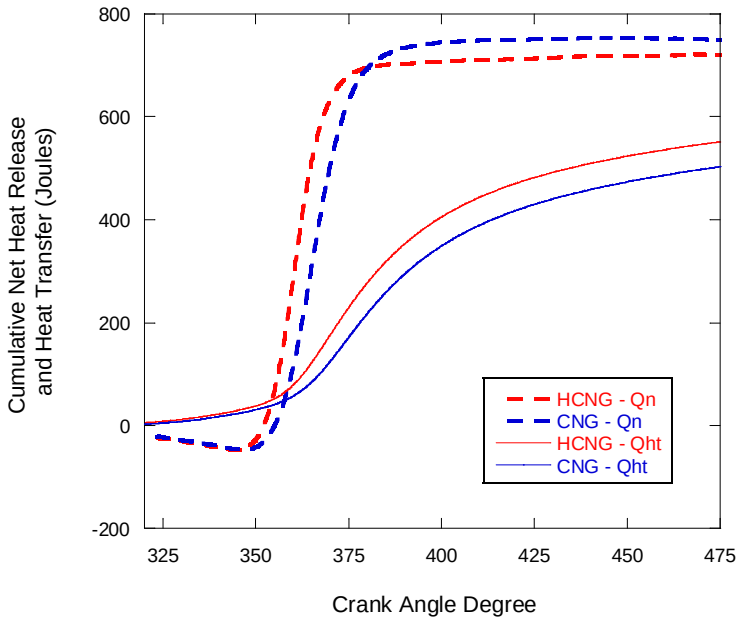

Figure **4-13**: Net Heat Release and Heat Transfer 1370 RPM, 30 hp Road Load

4.3.4 Coefficient of Variance

Reduction in coefficient of variance of indicated mean effective pressure (COV) is one of the main advantages of hydrogen addition to natural gas. This study recorded the values of COV at all test conditions. All values fell within the acceptable limits of engine stability. All conditions reported a COV of less than 2.5. The data shows that there is no advantage of COV with HCNG under these near stoichiometric combustion conditions. Any variance in combustion was probably due to cylinder residuals, which fluctuated in composition and quantity, or because of poor throttle control by the driver during the testing sequence. Low coefficient of variance of around 1 percent has been

reported in the literature [15] during stoichiometric combustion of HCNG and CNG. The investigation in the COV of HCNG and CNG combustion is of interest for lean combustion conditions. With increasing the excess air, combustion stability decreases. Hydrogen has been shown to increase combustion stability at these conditions, but its effect is negated during stoichiometric combustion.

4.4 Combustion Trends

Hydrogen has been shown to assist combustion at lower loads and reduce combustion performance at higher loads [5, 15]. This section discusses combustion performance, which was evaluated at 30 miles per hour at various speeds and loads. The goal was to determine the effect of hydrogen on natural gas combustion under varying conditions. Three test points were acquired at transmission position “D” and “D1,” at road loads of 10, 20, and 30 horsepower.

4.4.1 Combustion Duration

Increased load on the vehicle increases the load on the engine. Road load increases can be from uphill conditions, accessory loads, or road conditions. As the load increases, the rate of combustion increases rapidly because more fuel must be burned in the combustion cycle to produce the same power output. To produce the same amount of output from the cylinder, the engine must increase injection time in order to inject more fuel into the cylinder. Hydrogen content of 33 percent in natural gas represents only 9

percent of the fuel energy, which means some power is lost when using HCNG due to the reduction of volumetric energy content.

Figure **4-14** demonstrates the effects of hydrogen during a significant load increase on the engine. As the engine load increases, overall combustion duration decreases. According to scan tool data, the load on the engine during a road load of 10, 20 and 30 horsepower is 40, 57 and 66 percent, respectively, of wide-open throttle. As the load on the engine increases significantly from 40 to 67 percent throttle, reduction in combustion duration with hydrogen addition is reduced.

Figure **4-15** shows high-speed tests in which HCNG reduces combustion duration. High engine speed maximizes HCNG speed reduction [11]. Hydrogen addition at these high combustion duration points reduces the crank angle interval covered by 25 percent. The engine load conditions at this transmission position are 35, 40 and 43 percent wide-open throttle. At these small engine load increases, the combustion duration does not change significantly.

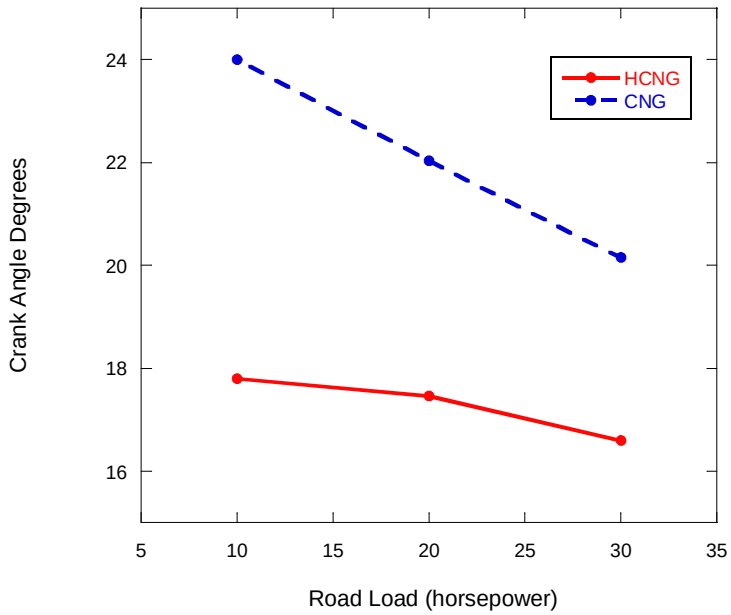

Figure **4-14**: Combustion Duration at 1350, 1360 and 1370 RPM

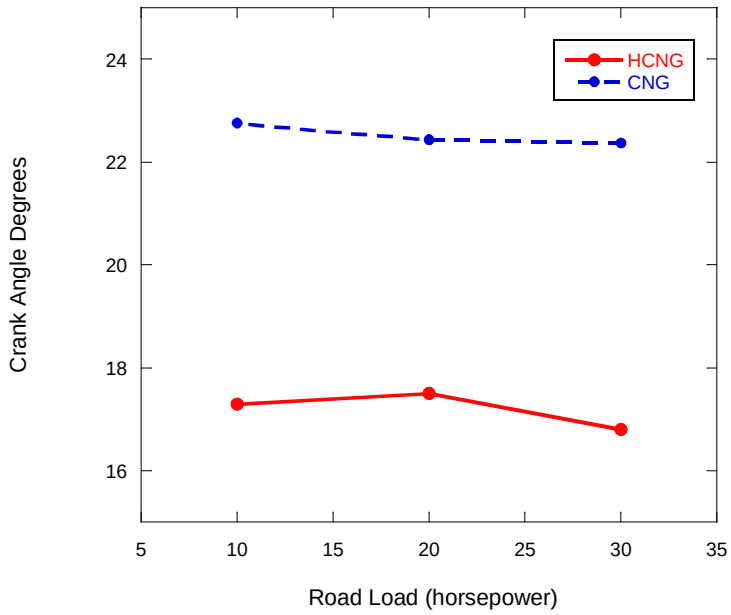

Figure **4-15**: Combustion Duration at 3700, 3750, 3800 RPM

4.4.2 Flame Development Angle

The flame development angle is the distance from the spark to when 10 percent of the mass of the fuel has burned [11]. Increasing hydrogen addition has proven to decrease the flame development angle in the literature [4]. This early stage of combustion features a mostly laminar flame that forms a spherical flame kernel around the spark plug gap. The flame interacts with the surrounding turbulent flow increasing the surface area of the flame, which increases the propagation speed of the flame. When hydrogen enters the flame kernel, its reaction with the flame front increases the speed at which the reaction zone propagates. Across all testing conditions, HCNG showed a reduction in flame development angle.

Figure **4-16** shows the decrease in flame development angle that occurred in these tests. As the engine load nears 67 percent of wide-open throttle, at a road load of 40 horsepower, the effects of hydrogen are reduced.

As with combustion duration, during high-speed conditions a decrease in the flame development angle is observed during HCNG combustion. This is shown in Figure **4-17**. For both indications of combustion speed, the effect of hydrogen addition in reducing flame development angle is more pronounced at higher speeds.

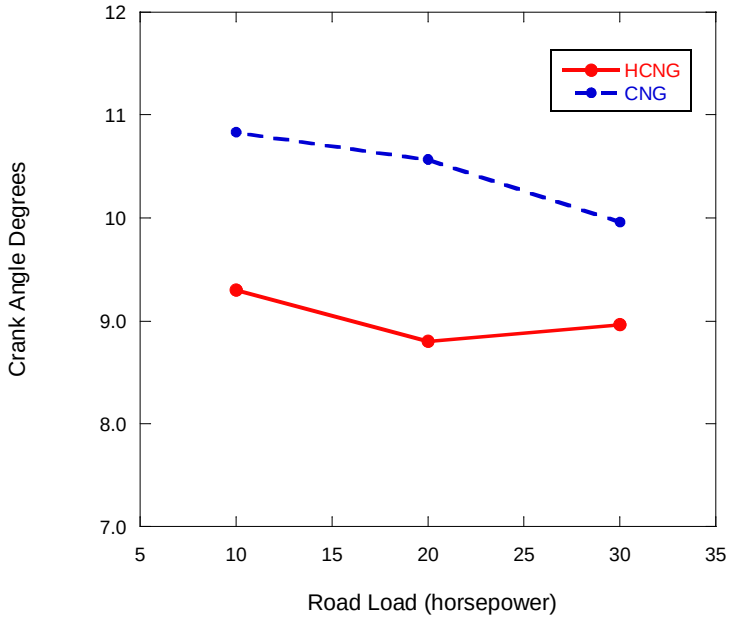

Figure **4-16**: Flame Development Angle at 1350, 1360 and 1370 RPM

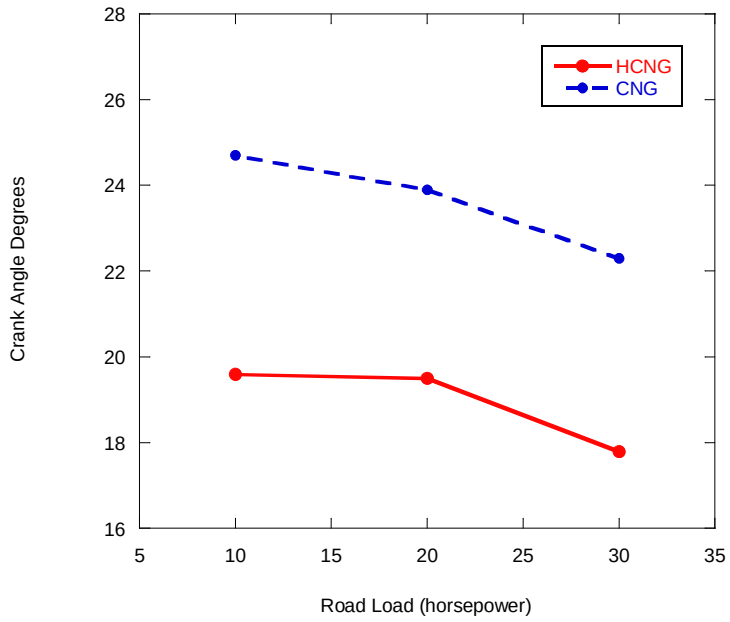

Figure **4-17**: Flame Development Angle at 3700, 3750, 3800 RPM

4.4.3 Indicated Thermal Efficiency

Spark-ignition engines use a throttle plate to control engine power. As the throttle plate closes, intake pressure and fuel flow are reduced, resulting in lower intake pressures. These lower pressures contribute to combustion inefficiencies. This effect is clearly seen in Figure **4-18,** which illustrates how load increases the thermal efficiency of the engine. The values obtained for indicated thermal efficiency in natural gas engines range from 33 to 38 percent, which is 10 percent higher than that obtained in gasoline spark-ignited engines. The main factor accounting for this discrepancy is that natural gas engines tend to have a higher compression ratio, which increases the thermal efficiency, and inaccuracy of mass measurements from instrumentation can reduce the theoretical energy available.

Many papers cite hydrogen addition as increasing the indicated thermal efficiency of natural gas [4, 35], however Figure **4-18** shows that compressed natural gas has a higher thermal efficiency than HCNG at all loads. While the data shows a deviation from expected thermal efficiency results, it is similar to results found by Bauer et al. [1] when testing an engine running at 700 and 900 rpm. The reduced thermal efficiency observed in this study is a result of the extra heat lost during high temperature combustion of HCNG and increased losses in indicated work due to early combustion. Improvement in thermal efficiency would be observed if EGR was reconnected or spark timing was retarded.

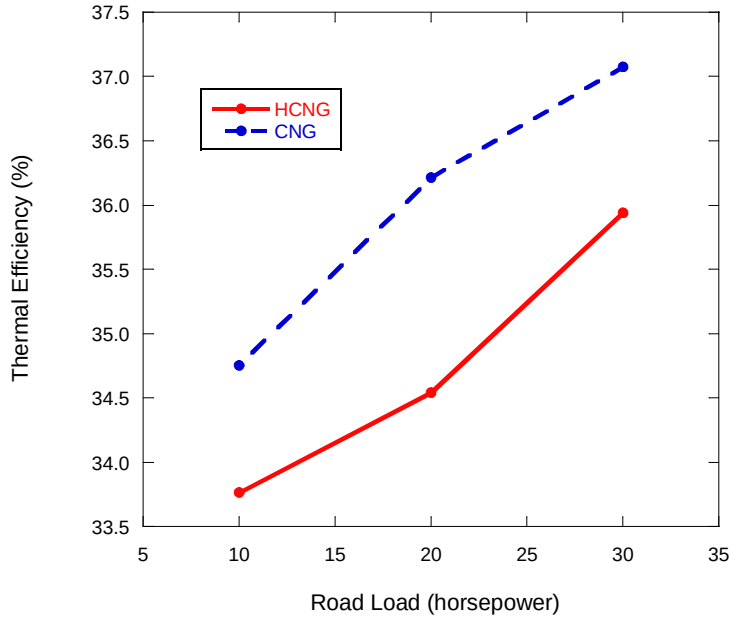

Figure **4-18**: Indicated Thermal Efficiency at 1350, 1360 and 1370 RPM

4.5 Emissions Results

The reduction of regulated pollutants is one of the main motivations for HCNG research. In this study, the engine-out exhaust measurements were recorded to determine the pre-catalyst effect of hydrogen addition on natural gas combustion. It was not possible to accurately record the actual load on the engine so the results can only be compared at the same testing conditions.

4.5.1 Carbon Dioxide

Carbon dioxide (CO_2) is a product of complete combustion. Figure **4-19** shows the CO_2 emissions present in the exhaust during this study. It was found that a reduction

of carbon-based fuel in the charge reduces the CO_2 formation by 10 percent. Reductions in CO_2 were independent of increased load. Natural gas fuel contains approximately 7.2 percent more carbon per unit energy than the HCNG used in the study. The engine-out CO_2 differences between the fuels corresponded with the amount of carbon oxidized in the combustion process.

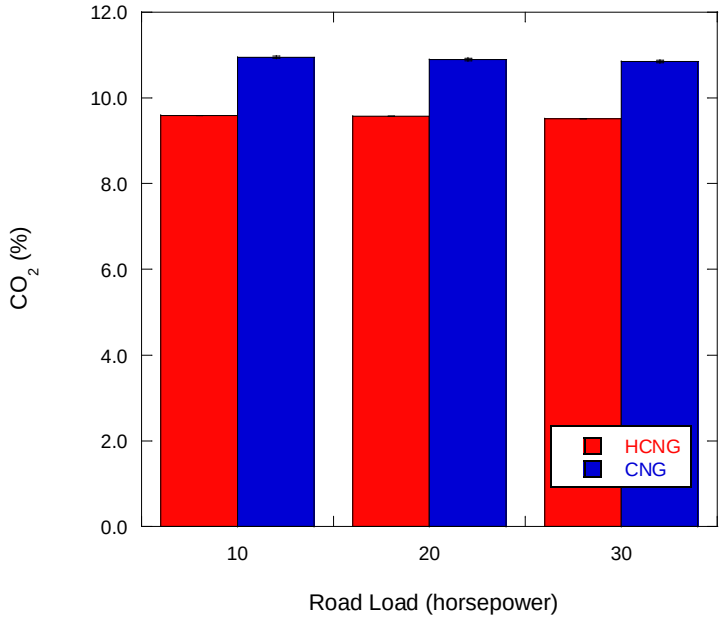

Figure **4-19**: CO_2 at 1350, 1360 and 1370 RPM

4.5.2 Carbon Monoxide Emissions

Carbon monoxide (CO) emissions are produced in high amounts during part load conditions due to incomplete oxidation. Decreased CO emissions have been observed by Andersson [15] at stoichiometric conditions. Figure **4-20** shows the carbon monoxide emissions produced over increasing loads. CO oxidation was enhanced by the higher

temperatures of the postflame gases during HCNG combustion. While reductions in CO concentration are seen with hydrogen addition, the results are statistically insignificant due to the range covered by the error bars. Therefore no conclusions can be drawn.

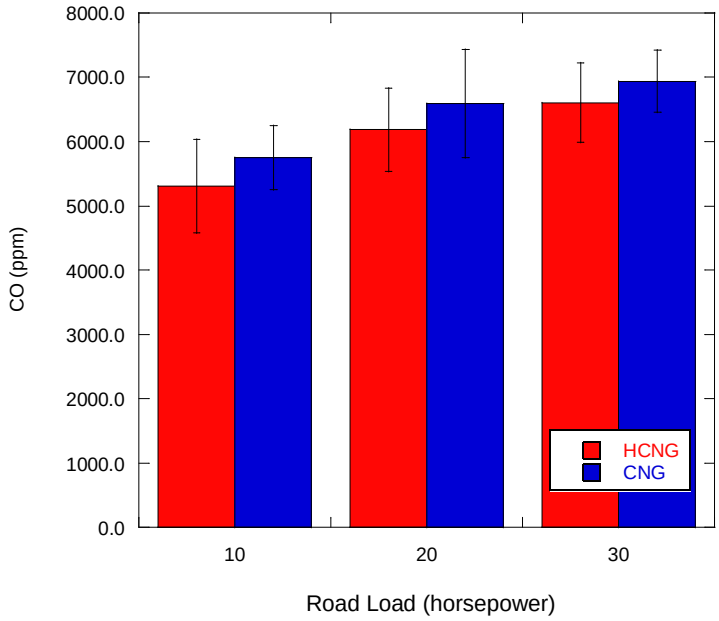

Figure **4-20**: CO at 1350, 1360 and 1370 RPM

4.5.3 Oxides of Nitrogen

High temperatures that occur during combustion are the main contributor to nitric oxide (NO) formation. In this study, the test vehicle controlled the air-fuel ratio to run stoichiometrically, which increased peak temperatures over lean-burn combustion. These higher temperatures were amplified by the hydrogen addition. Increased exposure to these post-combustion temperatures drove NO production, as shown in Figure **4-21**. An

increase in engine-out oxides of nitrogen emissions with HCNG has also been observed in the literature [5, 15, 22].

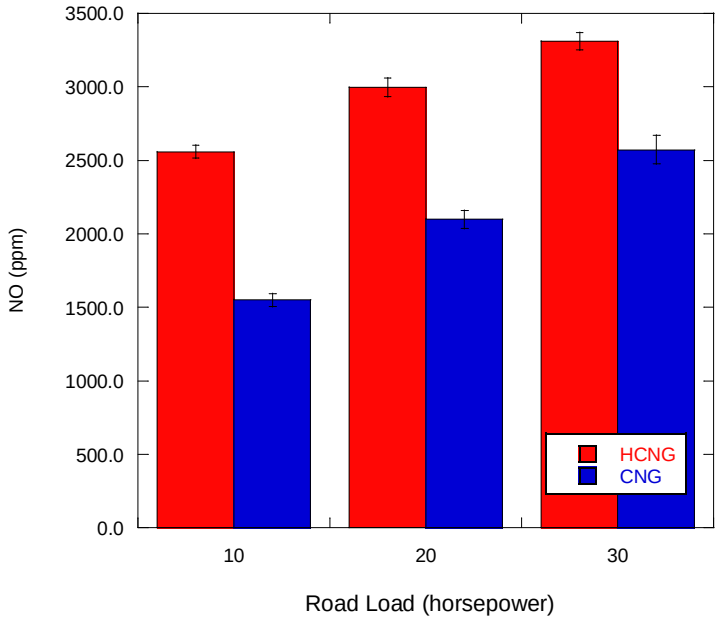

Figure **4-21**: NO at 1350, 1360 and 1370 RPM

4.6 Vehicle Speed

Two different vehicle speeds of 15 and 30 miles per hour were measured to determine the effect that speed has on combustion performance. After all of the calculations were performed, combustion performance in the cylinder when the vehicle is traveling at 15 miles per hour is nearly identical to when it is travelling at 30 miles per hour. Table **4-2** shows the engine load as a percentage of wide open throttle according to the ECU. Vehicle tests run at 15 miles per hour have a slightly lower load than the tests run at 30 miles per hour. Combustion trends are very similar at the same load

positions. The trends observed during increased loading conditions already have been addressed during this study and are not reported in detail in this section.

Table **4-2**: Road Load at Low Speed Test Settings

Road Load (hp)	15 mph Load (%)	30 mph Load (%)
10	38.00	42.00
20	53.00	57.00
30	58.00	65.00

Chapter 5

Conclusions and Future Work

5.1 Conclusions

Based on engine testing and simulation results, the following conclusions were drawn:

1. Stoichiometric combustion of HCNG reduces ignition delay and creates conditions conducive for a faster burn.

2. HCNG reacts faster than natural gas, producing a decrease in combustion duration. Apparent heat release rates are advanced which work against the motion of the piston.

3. Bulk cylinder temperatures of HCNG increase energy losses to the surroundings.

4. Work against the piston and heat transfer to the surroundings reduces thermal efficiency of HCNG compared with CNG.

5. The effects of hydrogen addition, (i.e., decreased flame development angle and combustion duration, increased temperatures, increased heat loss), decrease as the load on the engine increases.

6. At the same road load, changes in vehicle speed only slightly reduce the load on the engine, resulting in similar combustion performance.

5.2 Future Work

During this study, combustion performance was measured in the vehicle with no modifications except for fuel to determine the effect of hydrogen in natural gas combustion in a vehicle. Limits due to insufficient resources prevented measurement of fully functional combustion performance in the vehicle. For a more in-depth study, the following suggestions for future work are proposed.

1. Reprogram the ECU to optimize the engine to run based on the test fuel for combustion comparison.
2. Increase measuring equipment on the vehicle to measure actual operating conditions including EGR, fuel rail pressures to understand in-cylinder combustion processes better.

Bibliography

[1] C. G. Bauer and T. W. Forest, "Effect of hydrogen addition on the performance of methane-fueled vehicles. Part I: effect on S.I. engine performance," *International Journal of Hydrogen Energy*, vol. 26, pp. 55-70, 2001.

[2] P. Forster and V. Ramaswamy, "Changes in Atmospheric Constituents and in Radiative Forcing," in *Changes in Atmospheric Constituents and in Radiative Forcing. In: Climate Change 2007: The Physical Science Basis. Contribution of Working Group I to the Fourth Assessment Report of the Intergovernmental Panel on Climate Change*: Cambridge University Press, Cambridge, United Kingdom and New York, NY, USA., 2007.

[3] T. Truett, "Literature Review for the Baseline Knowledge Assessment of the Hydrogen, Fuel Cells, and Infrastructure Technologies Program," O. R. N. Laboratory, Ed., 2003.

[4] M. R. Swain, M. J. Yusef, Z. Dulger, and M. N. Swain, "The Effects of Hydrogen on Natural Gas Engine Operation," *Society of Automotive Engineers Paper No. 932775*, 1993.

[5] A. Cattelan and J. Wallace, "Exhaust Emission and Energy Consumption Effects from Hydrogen Supplementation of Natural Gas," in *Fuel & Lubricants Meeting & Exposition* Toronto, Ontario: *Society of Automotive Engineers Paper No. 960858*, 1995.

[6] I. Glassman, *Combustion*, 3rd ed.: Academic Press, Inc, 1996.

[7] "Hydrogen Commerce," http://www.hydrogencommerce.com, Accessed January, 2008.

[8] A. L. Dicks, "Hydrogen Generation from Natural Gas for the Fuel Cell Systems of Tomorrow," *Journal of Power Sources*, vol. 61, pp. 113-124, 1996.

[9] D. Guro, "Development of a Turnkey H2 Refueling Station," Air Products and Chemicals, Inc, Allentown, PA 2006.

[10] S. O. Akansu, Z. Dulger, N. Kahraman, and T. N. Veziroglu, "Internal combustion engines fueled by natural gas-hydrogen mixtures," *International Journal of Hydrogen Energy*, vol. 29, pp. 1527-1539, 2004.

[11] J. Heywood, *Internal Combustion Engine Fundamentals*: McGraw-Hill, Inc., 1988.

[12] P. M. Najt and T. Kuo, "An Experimental and Computational Evaluation of Two Dual-Intake-Valve Combustion Chambers," *Society of Automotive Engineers Paper No. 902140*, 1990.

[13] K. M. Chun and J. Heywood, "Estimating Heat-Release and Mass-of-Mixture Burned from Spark-Ignition Engine Pressure Data," *Combustion Science and Technology*, vol. 54, pp. 133-143, 1987.

[14] M. J. Zucrow, *Gas Dynamics* vol. 1. New York: John Wiley & Sons, 1976.

[15] T. Andersson, "Hydrogen Addition for Improved Lean Burn Capability on Natural Gas Engine," Lund Institute of Technology 2002.

[16] G. Yu, C. K. Law, and C. K. Wu, "Laminar Flame Speeds of Hydrocarbon + Air Mixtures with Hydrogen Addition," *Combustion and Flame,* pp. 339-347, 1985.

[17] K. Collier, N. Mullian, D. Shin, and S. Brandon, "Emission Results from the New Developments of a Dedicated Hydrogen-Enriched Natural Gas Heavy Duty Engine," Society of Automotive Engineers, 2005.

[18] S. Priyadarshi, "Effects of Hydrogen Enrichment on Methane/Air Premixed Laminar Flames Under SI Engine Conditions," in *Mechanical and Nuclear Engineering*. vol. Master of Science State College: The Pennsylvania State University, 2006, p. 128.

[19] P. Dagaut and A. Nicolle, "Experimental and detailed kinetic modeling study of hydrogen-enriched natural gas blend oxidation over extended temperature and equivalence ratio ranges," *Proceedings of the Combustion Institute,* vol. 30, pp. 2631-2638, 2005.

[20] R. W. Schefer, "Hydrogen Enrichment for improved lean flame stability," *International Journal of Hydrogen Energy,* vol. 28, pp. 1131-1141, 2003

[21] D. Karner and J. Francfort, "Dodge Ram Wagon Van – Hydrogen/CNG Operations Summary," U. S. D. o. Energy, Ed.: Idaho National Engineering and Environmental Laboratory, 2003.

[22] B. Nagalingam, F. Duebel, and K. Schmillen, "Performance Study Using Natural Gas, Hydrogen-Supplemented Natural Gas and hydrogen in AVL Research Engine," *International Association for Hydrogen Energy,* vol. 8, pp. 715-520, 1983.

[23] K. Collier, R. L. Hoekstra, N. Mulligan, C. Jones, and D. Hahn, "Untreated Exhaust Emissions of a Hydrogen-Enriched CNG Production Engine Conversion," in *International Congress & Exposition* Detroit, Michigan: Society of Automotive Engineers, 1996.

[24] G. A. Karim, I. Wierzba, and S. Boon, "Some Considerations of the Lean Flammability Limits of Mixtures Involving Hydrogen," *International Journal of Hydrogen Energy,* vol. 10, pp. 117-123, 1985.

[25] T. K. Jensen and J. Schramm, "Hydrocarbon Emissions from Combustion of Mixtures of Natural Gas and Hydrogen Containing Producer Gas in a SI Engine," *Society of Automotive Engineers Paper No. 2001-01-3532,* 2001.

[26] G. Pede, E. Rossi, M. Chiesa, and F. Ortenzi, "Test of Blends of Hydrogen and Natural Gas in a Light-Duty Vehicle," *Society of Automotive Engineers Paper No. 2007-01-2045,* 2007.

[27] C. Anastatia and G. Pestana, "A Cylinder Pressure Sensor for Closed Loop Engine Control," *Society of Automotive Engineers Paper No. 870288,* 1987.

[28] M. Hubbard, P. D. Dobson, and J. D. Powell, "Closed Loop Control of Spark Advance Using a Cylinder Pressure Sensor," *Journal of Dynamics Systems,* 1976.

[29] J. Y. Wong, *Theory of Ground Vehicles*, Second ed.,Wily-Interscience, 1993.

[30] "U.S. DOE Energy Efficiency and Renewable Energy Home Page," http://www.do.gov, Accessed January 2008.

[31] Melanie Fox, personal communication, 2008.

[32] T. K. Hayes, L. D. Savage, and S. C. Sorenson, "Cylinder Pressure Data Acquisition and Heat Release Analysis on a Personal Computer," *Society of Automotive Engineers Paper No. 860029,* 1986.

[33] R. Spindt, "Air-Fuel Ratios From Exhaust Gas Analysis," *Society of Automotive Engineers Paper No. 650507,* 1965.

[34] F. Ament, D. J. Patterson, and A. Mueller, "Heat Balance Provides Insight into Modern Engine Fuel Utilization," *SAE paper 770221,* 1977.

[35] R. Sierens and E. Rosseel, "Variable Composition Hydrogen/Natural Gas Mixtures for Increased Engine Efficiency and Decreased Emissions," *Journal of Engineering for Gas Turbines and Power,* vol. 122, pp. 135-140, 2000.

Appendix A

Fuel Properties

A.1 Natural Gas Composition

Table **A-1**: Natural Gas Composition

Natural Gas Constituents	% Volume
CH4	89.94
C2H6	5.26
C3H8	0.66
C4H10	0.05
H2	0.00
N2	4.08

A.2 Hydrogen-Natural Gas Composition

Table **A-2**: HCNG Composition

HCNG Constituents	% Volume
CH4	60.26
C2H6	3.53
C3H8	0.44
C4H10	0.04
H2	33.00
N2	2.74

A.3 Calculated Fuel Characteristics

Table **A-3**: Calculated Fuel Characteristics

	CNG	HCNG
Density (g/L)	0.7822	0.5538
LHV (kJ/kg)	46402	50358
Stoichiometric Air Fuel Ratio	17.18	18.10

Appendix B

Matlab Heat Release Code

B.1 Matlab Code programmed in version 2007b

```
% Program written by Jamie Clark, September 2007
% Updated February 1, 2008

% Program reads Pressure and Volume Data from pressure traces

% Data is taken to calculate heat release profile

clc
clear all

% read data files
input = dlmread ('C:\Documents and Settings\Jamie\Desktop\Tests
9_7_07\33','\t',1);

%test properties
speed = 1350; %speed in rpms
intakeAir = 110; %intake air degF
massair = 42.7; %mass flow of air in g/s

% fuel specific properties
afratio = 17.18; %air/fuel ratio of the mixture in cylinder
LHV = 46402; %lower heating value of fuel in kJ/kg
eqrat = 1.0; %equivalent ratio

%CALCULATIONS

% store the data from file in usable matrices
for i = 1:7200
    degCA(i) = input(i,1) + 0.1; % Crank angle position
    CylPres(i) = input (i,2); % In-cylinder Pressure
end

% engine properties
cyl = 8; %number of cylinders in the engine
bore = .09; % m
stroke = .106; % m
cr = 11; % compression ratio
conrod = .1691; % m - connecting rod length
crankrad = .053; % m
```

```
%DAQ properties
delCA = 0.1; %frequency of pressure measurements in degrees

% fuel specific initial conditions
gamma = 1.35; %initialized gamma
Cv = .897; %initialize Cv

% unit conversions
umassair = massair * 60 / 1000; %mass airflow conversion to kg/min
mair = umassair/cyl/(speed/2); % mass flow of air in kg
Tin = ((intakeAir - 32) * 5/9) + 273.15; %convert temp to Kelvin
R = 8.314/29*1000; %initialize R - J/kgK
rps = speed / 60; %engine speed in radians
sp = 2*stroke*rps; %mean piston speed
f = conrod/crankrad; % for heat transfer
mfuel = mair/afratio; %calculate mass of fuel

% Heat Transfer Calcs
C1 = 2.28; %constant c1 from Heywood
w = C1 * sp; % average flow velocity inside the cylinder for
compression and expansion - can add "+ C2*Vd*Tr/prVr*(Pcyl-Pmotored)"
Twall = 450; %assumed wall temperature in Kelvin

%Engine Volume calculations
Vd = pi*bore^2*stroke/4; %swept volume, displaced volume
Vc = Vd/(cr-1);%clearance volume

for i = 1:7200
    radCA(i) = degCA(i)*pi/180; % convert crank angle position to
radians
    cylVol(i) = Vc + (pi/4 * bore^2) * (crankrad*(1-
cos(radCA(i))+crankrad/(4*conrod)*(1-cos(2*radCA(i))))); %find volume
of cylinder
end

for i = 2:7199 %intermediate pressure smoothing and Net IMEP
    IntPres(i) = (CylPres(i-1) + CylPres(i+1))/2;
    dv(i) = (cylVol(i+1)-cylVol(i-1))/(2*delCA); %calculate dv
(m^3/deg)

    nimep(i) = (CylPres(i)+CylPres(i+1)) * dv(i);
    Nimep = sum(nimep)/2/Vd/10;

    if (i > 1800) && (i< 5400)
        gimep(i) = (CylPres(i)+CylPres(i+1))*dv(i);
        Gimep = sum(gimep)/2/Vd/10;
    end

    ica(i)=degCA(i);
end

for i = 3:7198
```

```
    Pres(i) = ((IntPres(i-1) + IntPres(i) + IntPres(i+1))/3); %smoothed
pressure trace
    Pres(i) = Pres(i)*100000; % convert bar to Pa
    kPres(i)= Pres(i)/1000; %Pressures in kPa
    pca(i) = degCA(i);
end

for i = 5:7195
    dp(i) = (-Pres(i+2)+8*Pres(i+1)-8*Pres(i-1)+Pres(i-2))/(12*delCA);
%calculate dp (Pa/deg)
    ppca(i) = degCA(i);
end

% Calc net IMEP

%initialize dq, T and Q
for i = 3:5436
    dq(i)= 0.0;
    Q(i)= 0.0;
    T(i)= Tin;
    T2(i) = Tin;
    tg(i) = Tin;
    Qtot = 0;
    done10 = 0;
    done50 = 0;
    done90 = 0;
    donesoc = 0;
    pair(i) = 0;
    Re(i) = 0;
    mu(i) = 0;
    Aw(i) = 0;
    hc(i) = 0;
    dQwall(i) = 0;
    Qwall(i) = 0;
    dQw(i) = 0;
    mb(i)=0;
    startmfb=0;
end

% temperature measurements
for i = 2000:5436

    % Calculate Heat Release
    if (i >= 3000) && (i <= 4950)
        dq(i) = (1/(gamma-1))*(gamma*Pres(i)*dv(i)+cylVol(i)*dp(i));
%solve Instantaneous Heat release J/deg
        Q(i) = dq(i)* delCA + Q(i-1); %Cumulative heat Release in J
    end

    % first temperature calculation
    dt(i) = 1/ ((mair + mfuel)*Cv)*((dq(i)/1000)-kPres(i)*dv(i));
%calculate change in temperature
    T(i) = dt(i) * delCA + T(i-1); %intergrate temp
```

```
    % second temperature calculation
    dt2(i) = 1/ ( (mair +((Q(i)/1000)/LHV))*Cv)*(dq(i)/1000 - kPres(i)
* dv(i));
    T2(i) = dt2(i) * delCA + T2(i-1);

    % third Temperature Caculation
    tg(i) = (Pres(i) * cylVol(i)) / (R * (mair + mfuel)) ; % ideal gas
law temperature calculation, gives highest #

    % Woschni heat transfer
    Aw(i) = (pi * bore ^ 2 / 2) + ((pi * bore * stroke / 2) * (f + 1 -
cos(radCA(i)) + (f ^ 2 - (sin(radCA(i))) ^ 2) ^ 0.5)); % area of wall
exposed unit of m2
    %pair(i) = Pres(i)/(R*tg(i)); % density of air
    %mu(i) = 3.3 * 10^-7 * tg(i) ^ 0.7/(1 + 0.027 * eqrat); %kg/msK
    %Re(i) = pair(i) * sp * bore / mu(i); %Renyolds number
    hc(i) = 3.26 * bore^-0.2 * (Pres(i)/1000)^0.8 * tg(i)^-0.55 *
w^0.8; % heat transfer coefficient in W/m2K pressure in kPa
    dQw(i) = hc(i) * Aw(i) * (T(i) - Twall) ; %J/s
    dQwall(i) = dQw(i) * (1/(360*rps)); % convert Watt to J/deg
    Qwall(i) = dQwall(i) * delCA + Qwall(i-1); % cumulative heat
transfer

    % recalculate gamma
    if T(i) > 1000
        gamma = 1.485 - 0.00025527 * T(i) + 1.3911e-7 * T(i)^2 -
3.6506e-11 * T(i)^3 + 3.6966e-15 * T(i)^4;
    else
        gamma = 1.3966 + 6.0455e-5 * T(i) - 1.5686e-7 * T(i)^2 -
5.6788e-11 * T(i)^3 + 9.2994e-14 * T(i)^4;
    end

    %crank angle referencing for plotting
    ca(i)=degCA(i);

    % recalculate Cv
    Cv = .287 / (gamma - 1);

    % calculate gross HR
    dQgross(i) = dq(i) + dQwall(i); %J/deg
    dmb(i) = dQgross(i)/(LHV*1000); % fuel burn rate kg/deg

    % Computation of total fraction burned (kg/deg)
    mb(i) = dmb(i) * delCA + mb(i-1);

    % Integrate to get total heat release
    Qgross(i) = Q(i) + Qwall(i);
end

%calculate MFB

for i = 3200:5000
```

```
    % convert Q to %
    maxQ = max(Q);
    minQ = min(Q);
    perQ(i) = (Q(i)-minQ) / (maxQ-minQ) * 100;

    %determine CA and Pressure at SOC, 10, 50 and 90% mfb
    if (perQ(i) == 0)
        startmfb = 1;
    end
    if (startmfb == 1)
         if (perQ(i) > 0) && (donesoc == 0)
            CAsoc = i/10;
            Psoc = kPres(i);
            donesoc = 1;
        elseif (perQ(i) >=10) && (done10 == 0)
            CAmfb10 = i/10;
            Pmfb10 = kPres(i);
            done10 = 1;
        elseif (perQ(i) >= 50) && (done50 == 0)
            CAmfb50 = i/10;
            Pmfb50 = kPres(i);
            done50 = 1;
        elseif (perQ(i) >= 90) && (done90 == 0)
            CAmfb90 = i/10;
            Pmfb90 = kPres(i);
            done90 = 1;
        end
    end
        mca(i)=degCA(i);
end

% combustion characteristics

tento90 = CAmfb90 - CAmfb10; %10 - 90 mfb
FDA = CAmfb10 - CAsoc; % flame development angle

% FDA = CAmfb10 - CAsoc; % flame development angle
%efficiencies

% DATA STORAGE & OUTPUT
% save values in matrix form


out(1,1) = max(Q); %J
out(2,1) = max(T); %K
out(3,1) = CAsoc; %CAD
out(4,1) = Psoc; %kPa
out(5,1) = CAmfb10; %CAD
out(6,1) = Pmfb10; %kPa
out(7,1) = CAmfb50; %CAD
out(8,1) = Pmfb50; %kPa
out(9,1) = CAmfb90; %CAD
```

```
out(10,1) = Pmfb90; %kPa
out(11,1) = FDA; %flame development angle, total CAD
out(12,1) = tento90; %total CAD
out(13,1) = max(dq); %J/deg
out(14,1) = max(dmb); %kg/deg
out(15,1) = Gimep; %kPa
out(16,1) = Nimep; %kPa

%output(18,1) = combeff;

dlmwrite('output.txt',out)
```